

# Multiple pulses of bimodal magmatism within the Hárrevárddo intrusion, Norrbotten County, Sweden

Dick Claeson & Ildikó Antal Lundin

april 2021

SGU-rapport 2021:20



Cover photo: View from the Hárrevárddo towards the Scandes.  
Photographer: Ildikó Antal Lundin

Author: Dick Claeson & Ildikó Antal Lundin

Head of unit: Ildikó Antal Lundin

Editor: Lina Rönnåsen

Geological Survey of Sweden  
Box 670, 751 28 Uppsala, Sweden  
phone: 018-17 90 00  
e-mail: [sgu@sgu.se](mailto:sgu@sgu.se)

[www.sgu.se](http://www.sgu.se)

## INNEHÅLL

Sammanfattning .....	4
Abstract .....	5
Introduction .....	5
Geological setting.....	6
Methods .....	11
Rocks of the Hárrevárddo intrusion .....	11
A lamprophyric dyke associated with the Hárrevárddo intrusion .....	15
Xenoliths of the Hárrevárddo intrusion.....	16
Petrography of some rocks of the Hárrevárddo intrusion.....	16
Internal contacts and magmatic flow related structural elements of the Hárrevárddo intrusion .....	22
Contacts with the surrounding rocks and intrusion related metamorphism .....	22
Structural elements within and in surrounding rocks of the Hárrevárddo intrusion.....	24
Whole-rock geochemistry of rocks from the Hárrevárddo intrusion .....	26
Petrophysics of rocks from the Hárrevárddo intrusion.....	29
Results of 2.5D forward gravity and magnetic modelling.....	30
Geophysical 3D modelling .....	32
Modelling 3D gabbroid to dioritoid bodies using the magnetic field .....	32
Modelling the 3D internal structure using the gravity field.....	34
Discussion.....	35
Shape of gabbroid-dioritoid bodies.....	35
Laccolith versus lopolith shape and form of incremental pulses of magma.....	36
Regional stress-field during emplacement and cooling.....	37
Conclusions .....	38
Acknowledgements .....	38
References.....	39

## SAMMANFATTNING

Undersökningsområdet för denna studie ligger söder om Kiruna, i den nordvästra delen av fennoskandiska skölden, i Norrbottens län. Hárrevárddointrusionen är en nyligen upptäckt strukturellt komplex intrusion, som ses som en mer än 500 km<sup>2</sup> stor, rund struktur bestående av flera intrusioner och magmatiska pulser, som alla har samma ålder. Tillsammans med den berggrund som finns utanför den cirkulära geofysiska avvikelserna – till största delen väster därom – och som tolkas vara av samma ålder eller något äldre, upptar området vid ytan mer än 800 km<sup>2</sup>. På berget Hárrevárddo – som ligger inom den stora, cirkulära anomalin – återfinns utmärkta blottningar av berggrunden, vilket ger möjlighet att studera de flesta av de olika magmatiska bergarterna och dess karaktär av multipla intrusiva pulser av olika sammansättningar. Därför döptes också hela det intrusiva komplexet till Hárrevárddo intrusionen.

Hárrevárddointrusionen uppvisar bimodal magmatism och saknar senare tektonisk överprägling i stor utsträckning. De vanligaste bergarterna varierar i sammansättning från granit till monzonit. Dessutom ses större partier med monzodiorit till gabbro. De flesta av bergarterna är kalifältspatporfyriska. En sällsynt lamprofyrgång förekommer inom intrusionen och hör troligen till samma magmatiska system.

Tredimensionell och 2.5D-modellering av magnetisk susceptibilitet och densitet används för att bedöma de olika geometrierna för bergarter som exponeras vid ytan. För att förklara intrusionens uppbyggnad kan den geofysiska 3D-modelleringen och dokumentationen tolkas som att på varandra följande, multipla injektioner av magmapulser med olika sammansättningar ägde rum. Flera inkrementella injektioner av olika storlekar av magma pulser föreslås för konstruktionen av Hárrevárddointrusionen från den geofysiska modelleringen, vilka formade en lopolitisk snarare än laccolitisk form på intrusionen. Pulserna av magma var troligen tabulära med tanke på vid vilket krustalt djup Hárrevárddointrusionen bildades. En ringstruktur med lagrad gabbro vid själva Hárrevárddo tolkas vara skapad i samband med en större tömning av en magmakammare, vilket fick till följd att en caldera och förkastningar skapades där den basiska magman kunde tränga upp. Vidare tolkas från observationerna och data att det fanns ett regionalt, syn-magmatiskt, extensionsrelaterat deformationssystem närvarande för cirka 1 780 miljoner år sedan.

Den här studien bidrar till vår kunskap om magmatiska processer beträffande hur magma intruderade i skorpan under paleoproterozoikum, sen-orosirium till tidig-staterium, och till vår kunskap om utvecklingen av magmatiska system.

## ABSTRACT

The focus area of this study is located south of Kiruna, in the north-western part of the Fennoscandian Shield, in the Norrbotten County, Sweden. The Hárrevárddo intrusion is a newly recognized structurally complex intrusion, which is seen as a more than 500 km<sup>2</sup>, round structure consisting of several pulses of magma, all of which are coeval. With the rocks outside the circular geophysical anomaly, for the most part to the west thereof, that are interpreted to be of the same age or just somewhat older, the area at the surface of these rocks occupies more than 800 km<sup>2</sup>. The best area with good exposures and the possibility to study most of the varieties of rocks within the large, circular anomaly and the multiple intrusive character is at the Hárrevárddo mountain and therefore the entire intrusion complex was named the Hárrevárddo intrusion.

The Hárrevárddo intrusion is bimodal in composition and lacks major later tectonic overprinting. The most common rock types range from granite-monzonite to monzodiorite-gabbro, where most are K-feldspar porphyritic. Rare lamprophyric dykes also occur.

We use 2.5 and 3-dimensional modelling of aeromagnetic and gravity data in order to assess the subsurface geometries of rocks exposed at the surface. The 3D geophysical modelling and field observations, litho-geochemistry, petrography presented suggest that the Hárrevárddo intrusion was constructed by intrusion of multiple pulses with a wide range of compositions. Several incremental injections of differently sized magma pulses are envisaged for the construction of the Hárrevárddo intrusion from the geophysical modelling, forming a lopolithic rather than laccolithic shape of the intrusion. The pulses of magma were probably tabular and not diapiric due to the crustal depth at which the Hárrevárddo intrusion formed. A ring structure with layered gabbro at the Hárrevárddo summit itself is interpreted to have been formed in connection with an emptying of a magma chamber, which resulted in formation of a caldera and faults being created in the crust, used as conduits for intrusion of the basic magma. Furthermore, the observations and data presented are interpreted to show that there was a regional, syn-magmatic, extension-related deformation in the study area c. 1780 Ma ago.

This study contributes to our knowledge of igneous processes regarding magma emplacement within the crust during the Paleoproterozoic (late-Orosirian to early-Statherian) and to the evolution of igneous systems.

**Keywords:** bimodal magmatism; emplacement processes; multiple pulses; 2.5D modelling; 3D density modelling; 3D magnetic susceptibility modelling

## INTRODUCTION

The structural compositions of granitoid and syenitoid intrusions and how they came to be assembled are yet not fully understood (e.g. Annen *et al.* 2015). Models involving ascent and emplacement are mostly based on the final shape and composition, i.e., the assembled, crystallised pluton, since there is no way to observe the actual magmas. Recent work indicates that not only diapirs may occur but also more complex scenarios involving rapid dyke-feeding (e.g. Gerbi *et al.* 2004), which may produce compositionally stratified plutons (e.g. Horsman *et al.* 2009, Burton-Johnson *et al.* 2016). Note that none of these cited papers indicate that large diapirs occur. The most probable way for magma to ascend are through dykes or along fractures (e.g. Vigneresse & Clemens 2000, Solano *et al.* 2012).

To advance our understanding of crustal magmatism, we need to determine what mechanisms govern the fluxes of magma into the crust and how the geometry and extent of magma pulses are controlled (e.g. Annen *et al.* 2015). Concentrically zoned granitoid and syenitoid plutons display

either normal or inverse zonation or a mix thereof. The Causerets-Panticosa granite complex (e.g. Debon 1980, Gleizes *et al.* 1998, Gil-Imaz *et al.* 2012) is a good example of normally zoned plutons, i.e. where the less differentiated rocks occur at the margins. Inverse zonation where less differentiated rocks occur in the central portion is less common or related to mingling and mixing (e.g. Délérís *et al.* 1996, Nédélec & Bouchez 2015).

Ancient syn-emplacement deformation related to the magmatic activity of granitoid and syenitoid intrusions are recorded as lineations, foliations, magmatic to submagmatic microstructures, magmatic shear zones, and magnetic fabrics (e.g. Délérís *et al.* 1996, Gleizes *et al.* 1998, Razanatseho *et al.* 2009). Tectonic lineations, foliations, microstructures, shear zones, and magnetic fabrics may form during or after the final formation.

The above examples and most studies of complex granitoid and syenitoid intrusions are from the Phanerozoic; here we present a Paleoproterozoic complex, the Hárrevárddo intrusion, and modelling its three-dimensional structure and thus its magmatic construction using a combination of geophysical and petrological data. Airborne magnetic and ground gravity data are available in the study area. Both the high resolution magnetic- and the gravity measurements were carried out by the Geological Survey of Sweden.

No previous mapping effort has recognized that the Hárrevárddo intrusion may be considered as a large or structurally complex intrusion, with associated bimodal magmatism (Claeson & Antal Lundin 2019).

## GEOLOGICAL SETTING

The study area is located south of Kiruna, in the north-western part of the Fennoscandian Shield, in the Norrbotten County, Sweden (fig. 1). The Precambrian crystalline bedrock is covered to the west by Ediacaran to Cambrian sedimentary rocks, and overthrust by rocks belonging to the Caledonian orogen (fig. 1). The Svecokarelian orogeny (2.0–1.8 Ga) in the area is associated with a convergent tectonic setting, during which volcanic and sedimentary rocks were formed and intruded by several generations of intrusive rocks. Several events of regional deformation, including major folding and shearing, occurred mostly under low to intermediate pressure and variable temperature metamorphic conditions. The Hárrevárddo intrusion is part of voluminous magmatism during the waning stages of the Svecokarelian orogeny in a continental arc-setting.

The large, circular magnetic anomaly that roughly covers 500 km<sup>2</sup> consists of multiple, coeval intrusions of bimodal magmatism, i.e. both basic rocks, gabbro to diorite and intermediate to acidic rocks; from quartz monzodiorite, quartz monzonite, to granite (fig. 1, 2). These rock types are intimately related to each other and there is no doubt based on field observations that all of them are coeval, since they all lack the metamorphic overprinting seen in older rocks (Antal Lundin *et al.* 2010, 2011, 2012a, 2012b, Claeson and Antal Lundin, 2013, 2015, 2019). On the magnetic anomaly map (fig. 2) the internal structure of the intrusion is characterised by varying levels of magnetization and the structure coincides with a moderate gravity high with local, internal variations derived from bedrock with different densities (fig.3, Antal Lundin *et al.* 2012a). The gravity field within the circular structure decreases to the north-west indicating occurrence of low-density rocks with acid compositions (fig. 3). The quartz monzodiorite, monzodiorite, and gabbroid to diorite rocks have high magnetic susceptibilities within the Hárrevárddo intrusion. Density determinations show that the quartz monzodiorite to monzodiorite have densities between 2 700 to 2 800 kg/m<sup>3</sup>, however a density of 2 700 kg/m<sup>3</sup> is sufficient to explain the moderately positive gravity anomaly in the eastern part of the structure (fig. 3 and Table 2). The best area with good exposures and the possibility to study most of the varieties of rocks within the large, circular anomaly and the multiple intrusive character is at the Hárrevárddo mountain

and therefore the entire intrusion complex was named the Hárrevárddo intrusion (Claeson & Antal Lundin 2019). The geophysical signature suggests a complex built multiple intrusion, with a diameter of c. 23 km, where the older supracrustal rocks found within the Hárrevárddo intrusion make the patterns even more complex, whereas the supracrustal rocks outside the intrusion clearly delineate the N, S, and E contacts. Within the delineated, nearly circular anomaly, a smaller circular pattern with a positive magnetic anomaly having a diameter of about 4.5 km appears at the location Hárrevárddo mountain and is interpreted as a “ring dyke” structure (fig. 1, 2). This, together with the variety of basic rocks coinciding with the smaller circular anomaly, shows that the more than 500 km<sup>2</sup> large, round structure consists of several pulses of magma. All varieties of rocks are interpreted as more or less of the same age because they lack metamorphic overprinting. There are rocks outside the Hárrevárddo intrusion, for the most part W of but some S and E of, that are interpreted to be of the same age and some possibly just a fraction older (Claeson & Antal 2019). Thus, the more or less coeval magmatism occupies more than 800 km<sup>2</sup> (fig. 1–3). A U-Pb zircon age determination of quartz monzonite at Jervas, which is associated with the typical, multiple rock types granite-monzonite-quartz monzodiorite-monzodiorite and well within the Hárrevárddo intrusion, resulted in an age of  $1\,784 \pm 4$  Ma (Claeson *et al.* 2018b). Its density is 2 742 kg/m<sup>3</sup> and the magnetic susceptibility measured on outcrops varies between 2 210 and  $6\,300 \times 10^{-5}$  SI units.

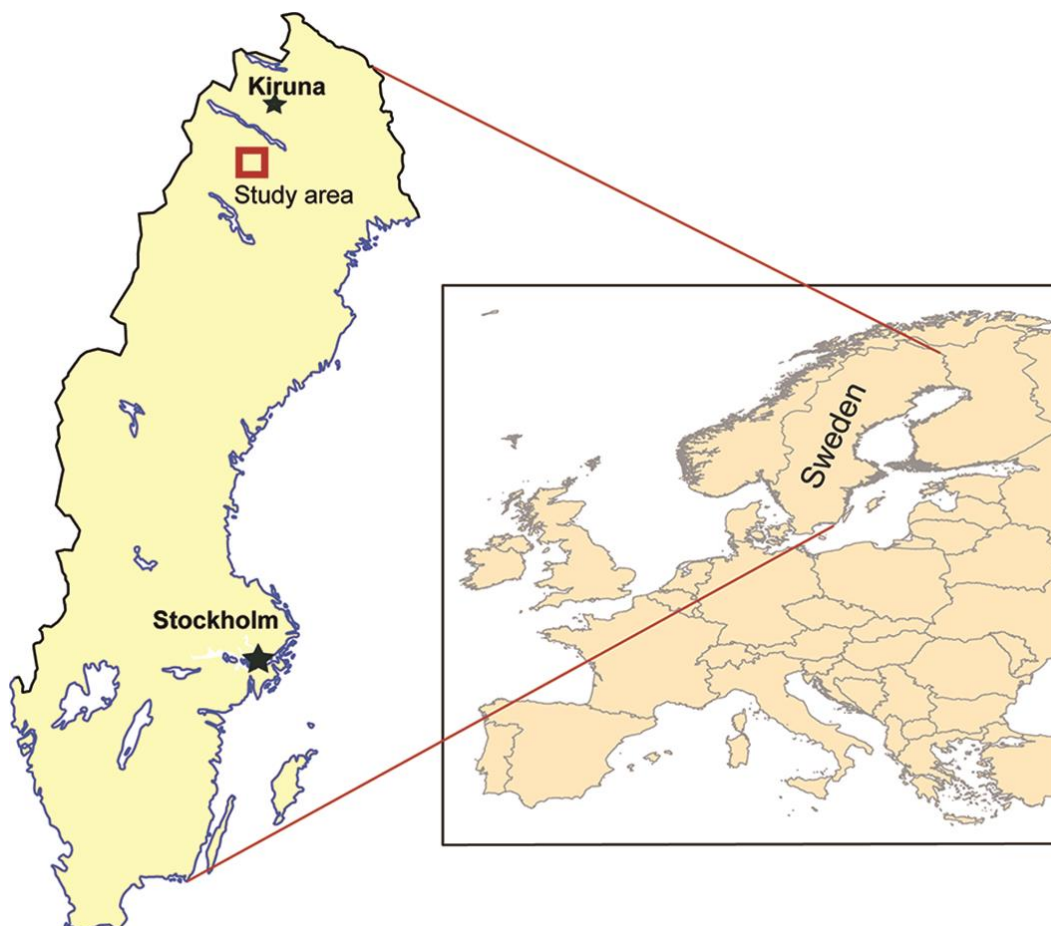


**Figure 1. A.** Location of the study area.

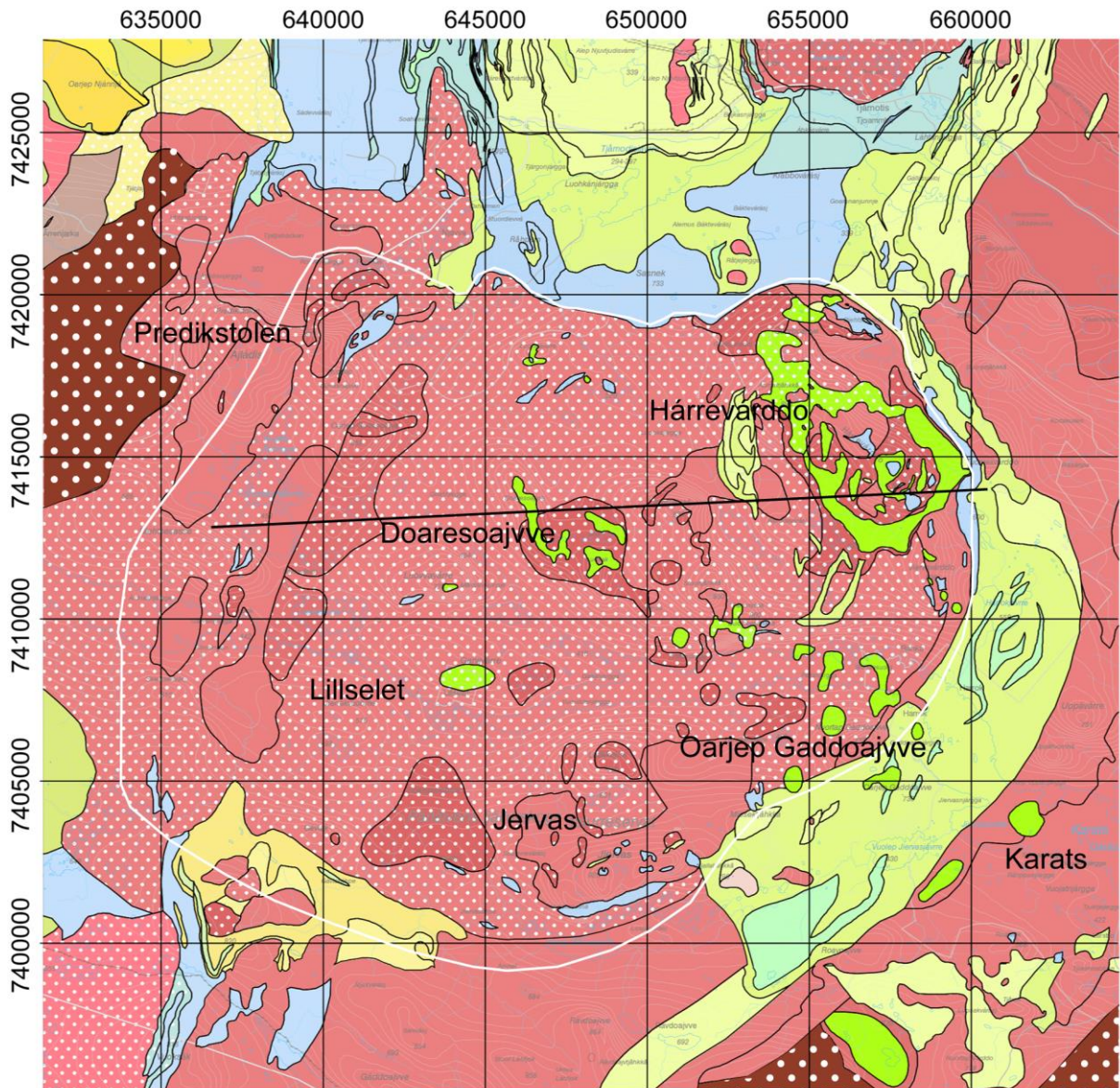


**Figure 1.** Continued. **B.** Bedrock map of the Hárrevárddo intrusion and surroundings. Coordinates in the Swedish national grid SWEREF 99TM. The white contour shows the outline of the circular part of the Hárrevárddo intrusion. The Hárrevárddo mountain is seen in the north-eastern part.

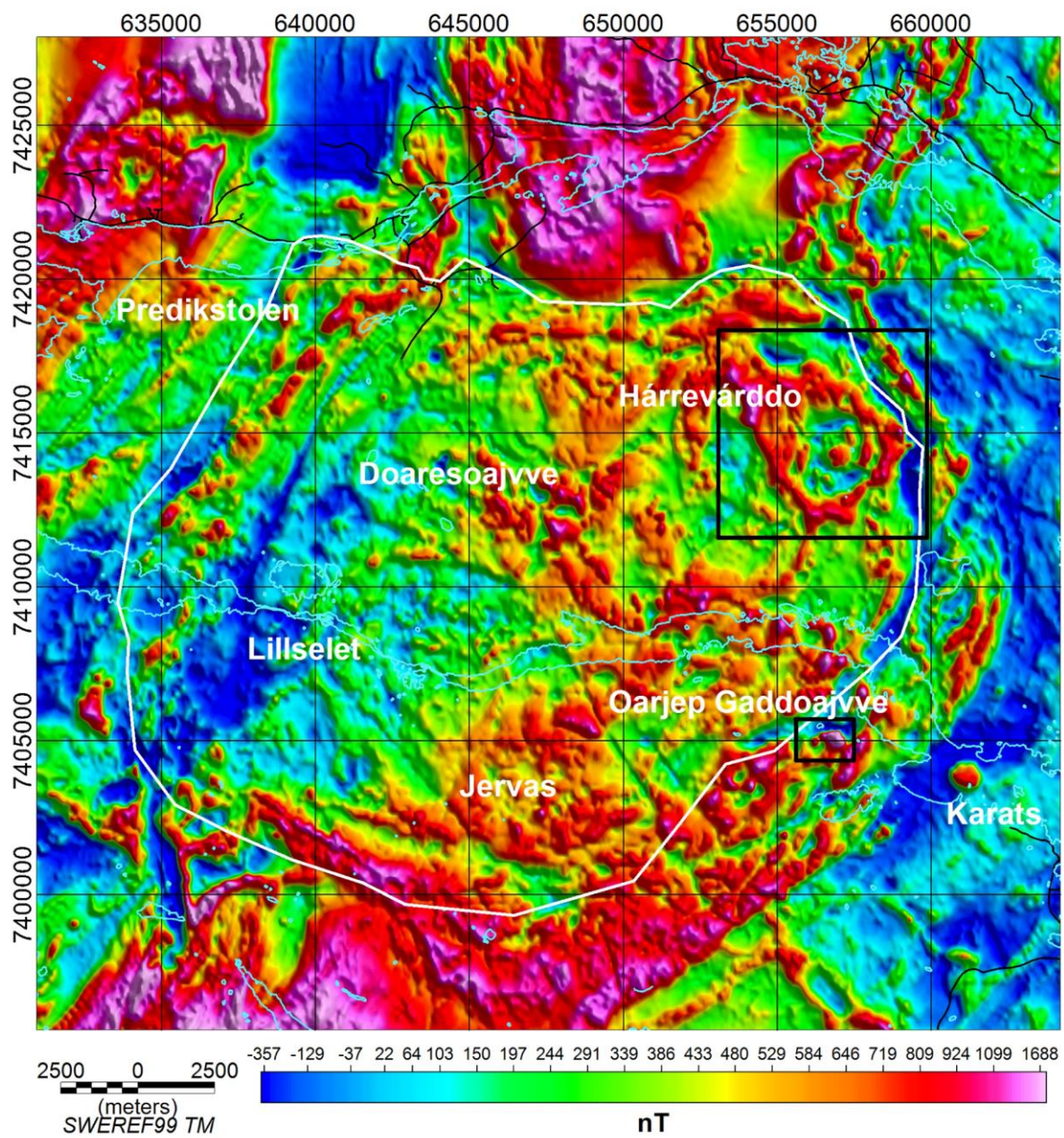


**Figure 2.** Magnetic anomaly map over the study area. The two black rectangles show the areas where 3D susceptibility models have been created. The white contour shows the outline of the circular part of the Hárrevárddo intrusion.

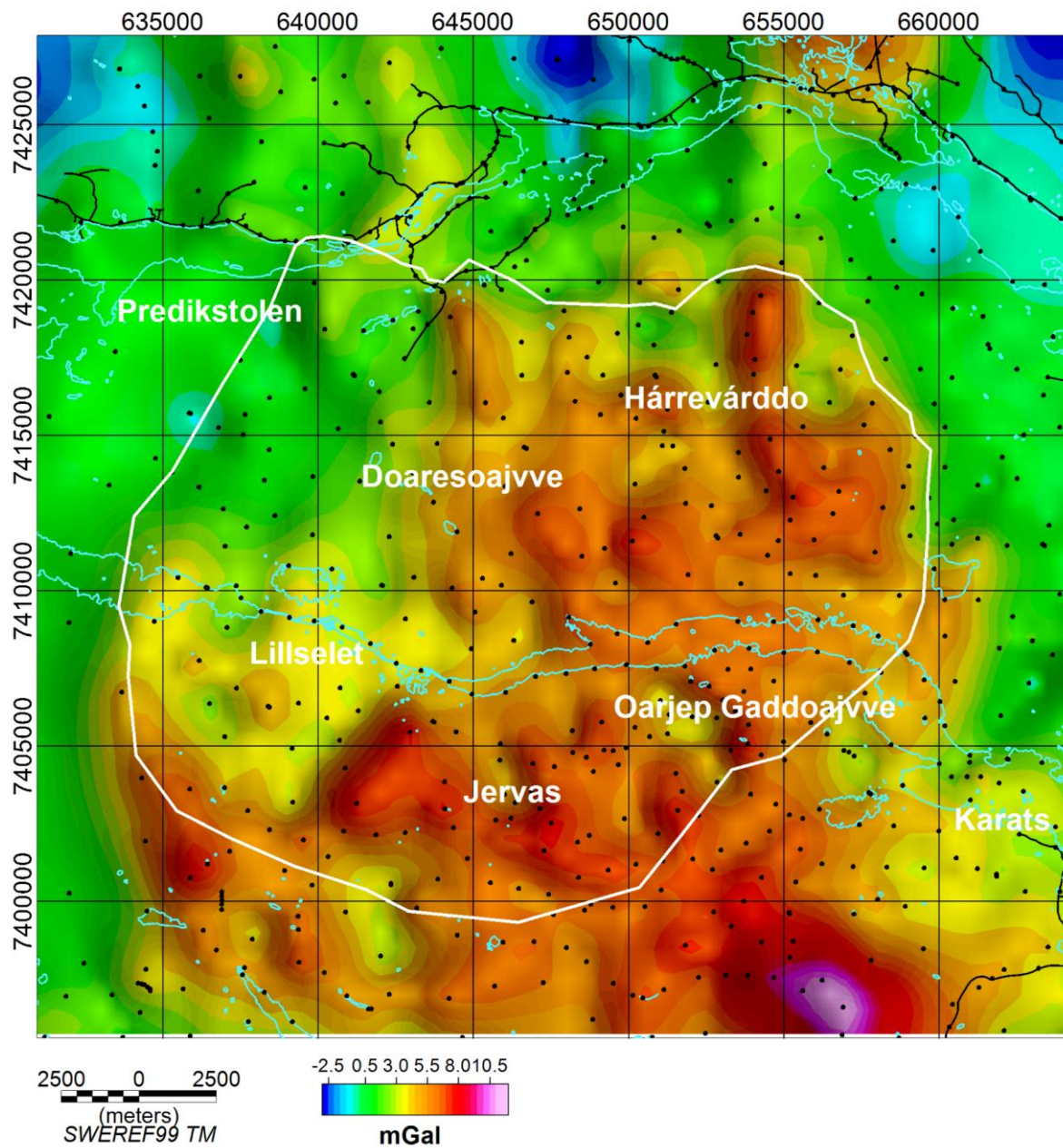


**Figure 3.** Residual gravity field over the study area. The gravity stations are shown by black dots and the white contour shows the outline of the circular part of the Hárrevárddo intrusion.

## METHODS

Airborne geophysical measurements over the area presented here were carried out in 2012 by SGU with a ground clearance at 60 m and a sampling interval of 16 m. The line distance was 200 m and the survey direction was east-west. The map over the magnetic field was produced using a grid cell size of 50 m.

Regional gravity measurements were conducted by SGU and LMV during different periods, most of the measurements were done between 1970 and 1985. New measurements were carried out 2010 and 2011 by SGU. The Bouguer anomaly is based upon the reference field RG83 (Regional Standard Network, 1982, the gravity formula from 1982, Bouguer density of 2 670 kg/m<sup>3</sup> and gravity database SW1510. The data were gridded using a grid cell size of 500 m. The distance between the measurement points varies between 300 to 3 000 m.

Petrophysical properties of different rock types from the Hárrevárddo intrusion are given in Table 2 and have been used to constrain the models.

3D density and susceptibility models were generated with inverse technique using the software Voxi. The Voxi program is a 3D finite difference inversion module by Geosoft Inc. In inverse modelling, measured data determines the geometry and physical properties of the geological structures. The space is divided into cells of known geometry and the physical properties of each cell are estimated using an iterative mathematical method (Aster *et al.* 2005). The models are constrained by known physical properties of the bedrock.

Li & Oldenburg (1996, 1998) described 3D inversion of potential field data in detail and pointed out the importance of the depth-weighting function to address the non-uniqueness of potential field inversions. Petrophysical data, such as magnetic susceptibility and density, were previously used by researchers to constrain model parameters.

The lithochemical analyses were performed at ALS Chemex using their analytical packages CCP-PKG01, ME-MS41, and PGM-ICP23. The petrophysical measurements were done in the petrophysics lab at the Geological Survey of Sweden (SGU).

## ROCKS OF THE HÁRREVÁRDDO INTRUSION

For the most part outcrops of the Hárrevárddo intrusion consists of red to greyish red K-feldspar porphyritic monzonite to granite, where the phenocrysts are usually 5–20 mm in size (5–30%), a few larger, in an otherwise medium- to coarse-grained matrix (fig. 4A). In the western part of the intrusion occurs massive, medium-grained to coarse-grained, K-feldspar porphyritic monzonite to quartz monzonite, which mainly distinguishes them by having grey phenocrysts, unlike similar rocks elsewhere within the anomaly that show a reddish tint.

The age determined rock at Jervas is an uneven-grained quartz monzonite that is undeformed, massive, and grey (Claeson *et al.* 2018b). It is medium- to coarse grained, and porphyritic with 10–20 mm sized phenocrysts of potassium feldspar (0–3%, fig. 4B, C).

Dark grey to reddish grey K-feldspar porphyritic monzodiorite, quartz monzodiorite to monzonite form larger continuous areas across the multiple intrusions. Phenocrysts are 5 to 20 mm in size (5–20%) in a medium- to coarse-grained matrix. Normally, they have up to 15–20% amphibole and biotite in the matrix, with amphibole clearly dominating. These rocks show in places a well-developed magmatic flow structure, where parallel-oriented phenocrysts and dark minerals constitute a magmatic foliation and sometimes even mineral lineation e.g. at Oarjep Guossoajve (fig. 4D).

Large areas of the Hárrevárddo intrusion comprise red to greyish red granite to quartz monzonite that is medium- to coarse-grained. Normally, none or only a few phenocrysts of potassium feldspar are present, and the main dark mineral is biotite. Excellent exposures of this quartz monzonite to granite occurs, e.g. in a large area at the Hárrevárddo mountain (fig. 4E, Antal Lundin *et al.* 2012a) and in an area at Sálastjáhkka and Stuortjáhkka with a typical appearance (fig. 4F).

There are areas of potassium feldspar porphyric quartz monzonite to quartz monzodiorite at Hárrevárddo (fig. 4G).

At the Hárrevárddo mountain there is a well-preserved mafic intrusion, “ring dyke” structure, displaying layering with easily weathered, moderately to high magnetic parts ( $1\ 350\text{--}4\ 000 \times 10^{-5}$  SI units) and more weathering resistant high-magnetic parts ( $6\ 000\text{--}15\ 000 \times 10^{-5}$  SI units, fig. 4H). There are also some ultramafic layers, dykes and fracture fillings of amphibole as well as gabbro pegmatoid parts (Antal Lundin *et al.* 2012a). The layering is seen as light and dark layers, variation in composition and grain-size differences. The gabbro is massive, black to dark grey, fine-grained to medium-grained. Pyroxene, amphibole, and biotite are present in the matrix. Areas of black to dark grey, K-feldspar porphyritic diorite to monzodiorite is also found at Hárrevárddo (Antal Lundin *et al.* 2012a) but appears to be spatially separated from the gabbro in today’s exposed parts and no field observation have shown their relationship. Most likely are these rocks derived from the gabbro through fractionation. Besides here, these two rock varieties occur at different locations within the Hárrevárddo intrusion. Winding but sharp contacts between gabbro and surrounding monzodiorite, quartz monzodiorite, and monzonite, without any signs of chilled margin effects, are interpreted to indicate that the rocks are more or less coeval in the sense of the lifespan of filling the Hárrevárddo intrusion (fig. 4I). This is also true for granite at the Hárrevárddo mountain and the previously described quartz monzonite, monzonite, granite, quartz monzodiorite to monzodiorite present at Hárrevárddo (see above). All of these are interpreted to be of the same age as those determined at Jervas. However, it also implies that most of them were nearly fully crystallised but still hot enough for no chilled margins to form, when another batch or compositionally different magma arrived. Otherwise, magma mingling textures along contacts would most probably have been present.

In the area of the Doaresoajvve is a well-preserved gabbro present that shows winding and sharp contacts with granite to quartz monzonite without any signs of chilled margin and thus all rocks are interpreted as coeval. The gabbro is medium-grained to coarse-grained and contains up to 20 mm large phenocrysts of plagioclase (fig. 4J, Antal Lundin *et al.* 2012b).

Massive, brownish-grey to reddish-grey, medium-grained to coarse-grained monzodiorite is porphyritic with 5 to 25 mm large K-feldspar phenocrysts (2–8%) at Ganijvárre just north of Lillsalet (fig. 4K). Locally, gabbroid enclaves and mafic minerals accumulated as aggregates are observed (fig. 4L). At one locality at Ganijvárre, the monzodiorite exhibits well-developed magmatic flow structures with a shallow orientation, measured at 290/8 (RHR) of both parallel oriented phenocrysts and dark minerals (fig. 4M).

Magma mingling or mixing features other than coeval mafic enclaves were not observed during the surveying of the Hárrevárddo intrusion. Mafic enclaves are present at some outcrops but in general not observed as any large proportion of the more felsic rocks.

A layered gabbro occurs at Oarjep Gáddoajvve and is interpreted to be coeval with the Hárrevárddo intrusion. The gabbroid rocks at Oarjep Gáddoajvve are massive, well-preserved, and intruded older, surrounding volcanic rocks to the southeast (fig. 1, 2). At least two distinct varieties exist, a magnetite-rich and biotite-bearing gabbroid to dioritoid (fig. 4N), and a plagioclase-rich gabbroid to dioritoid (fig. 4O). The magnetite-rich magma or similar pulses possibly also entered parts within the multiple Hárrevárddo intrusion.

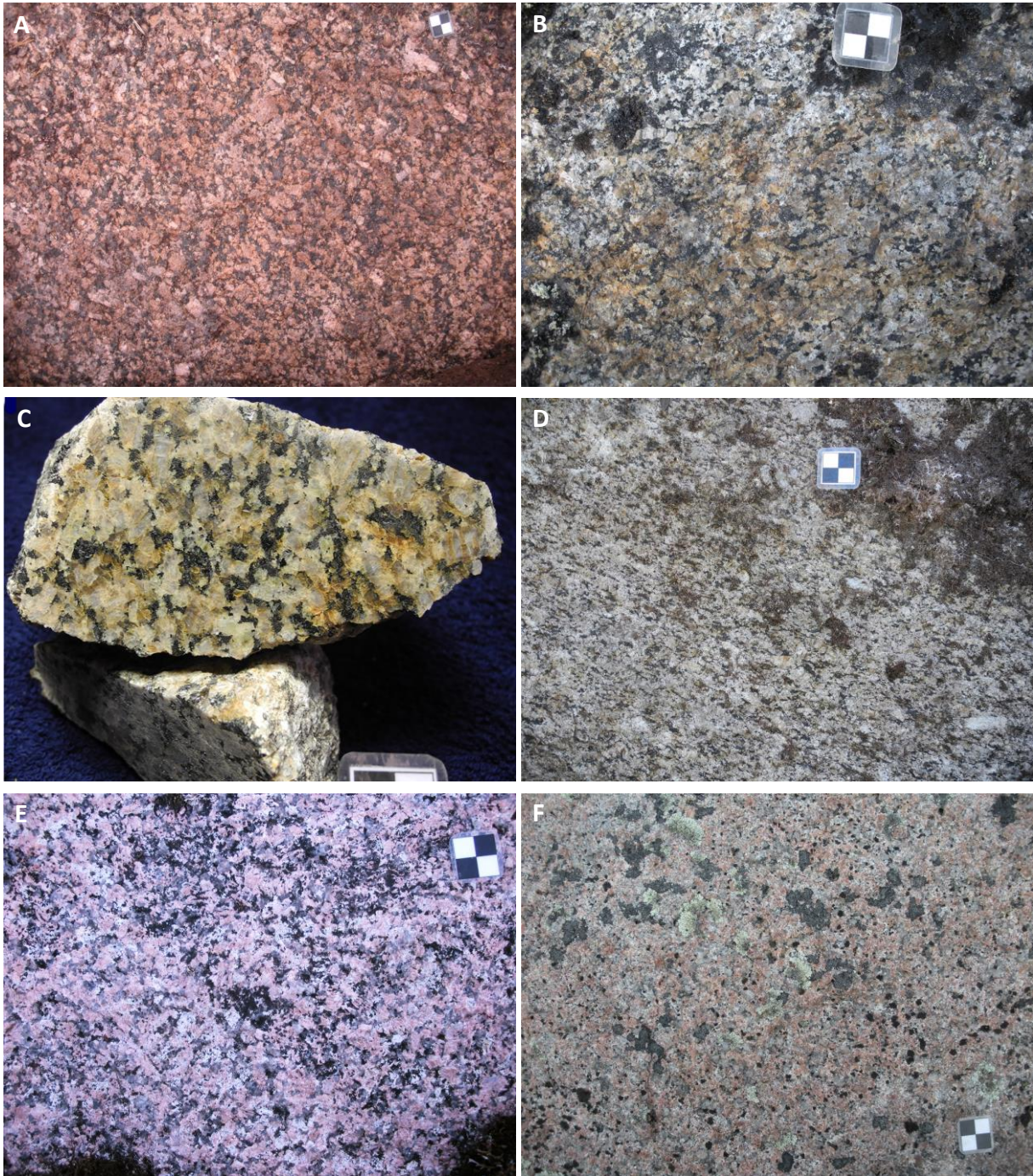


**Figure 4.** **A.** Massive, K-feldspar porphyritic monzonite to granite (7416282/648336). **B.** The age determined quartz monzonite at Jervas, **C.** cut and wetted (7403249/650222). **D.** K-feldspar porphyritic monzodiorite to monzonite with well-developed magmatic foliation at 25/50 RHR (7416245/ 640810). **E.** Massive, even-grained, coarse-grained, red to greyish red quartz monzonite to granite (7416312/655365). **F.** Massive, even-grained, red granite to quartz monzonite (7410873/651433).

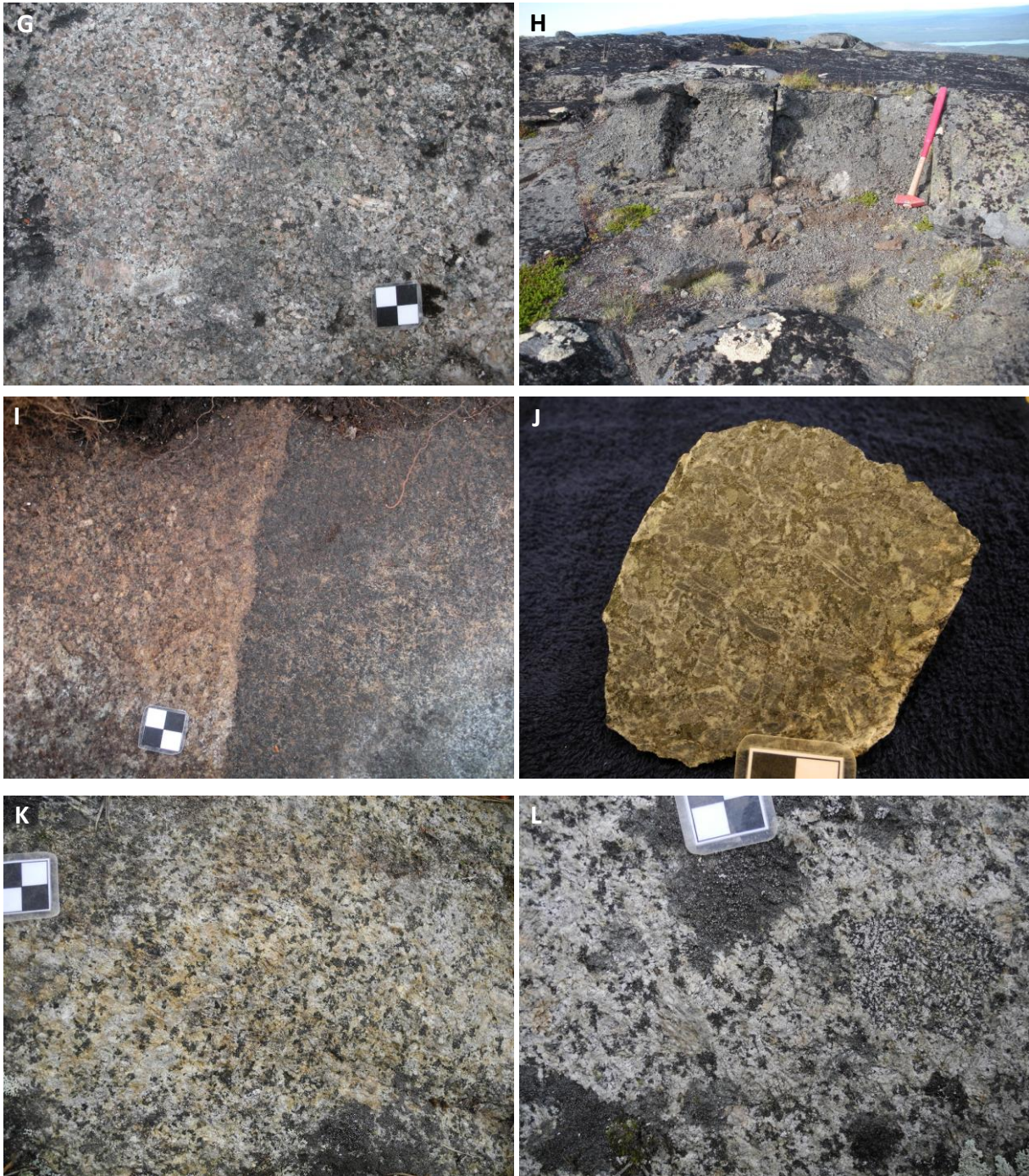


**Figure 4.** Continued. **G.** Potassium feldspar porphyritic quartz monzonite to quartz monzodiorite from Hárrevárddo (7414364/656970). **H.** Layered gabbroic rocks with easily weathered, moderately to high magnetic parts and more weathering resistant high-magnetic parts (7414486/657886). **I.** Winding but sharp contact between gabbro and monzodiorite to quartz monzodiorite (7414364/656970). **J.** Well-preserved gabbro containing up to 20 mm large phenocrysts of plagioclase, cut and wetted (7412949/645879). **K.** Potassium feldspar porphyritic monzodiorite to quartz monzodiorite (7408249/643510). **L.** Coeval mafic enclave in monzodiorite, darker and finer grained area to the right in image (7408199/643150).

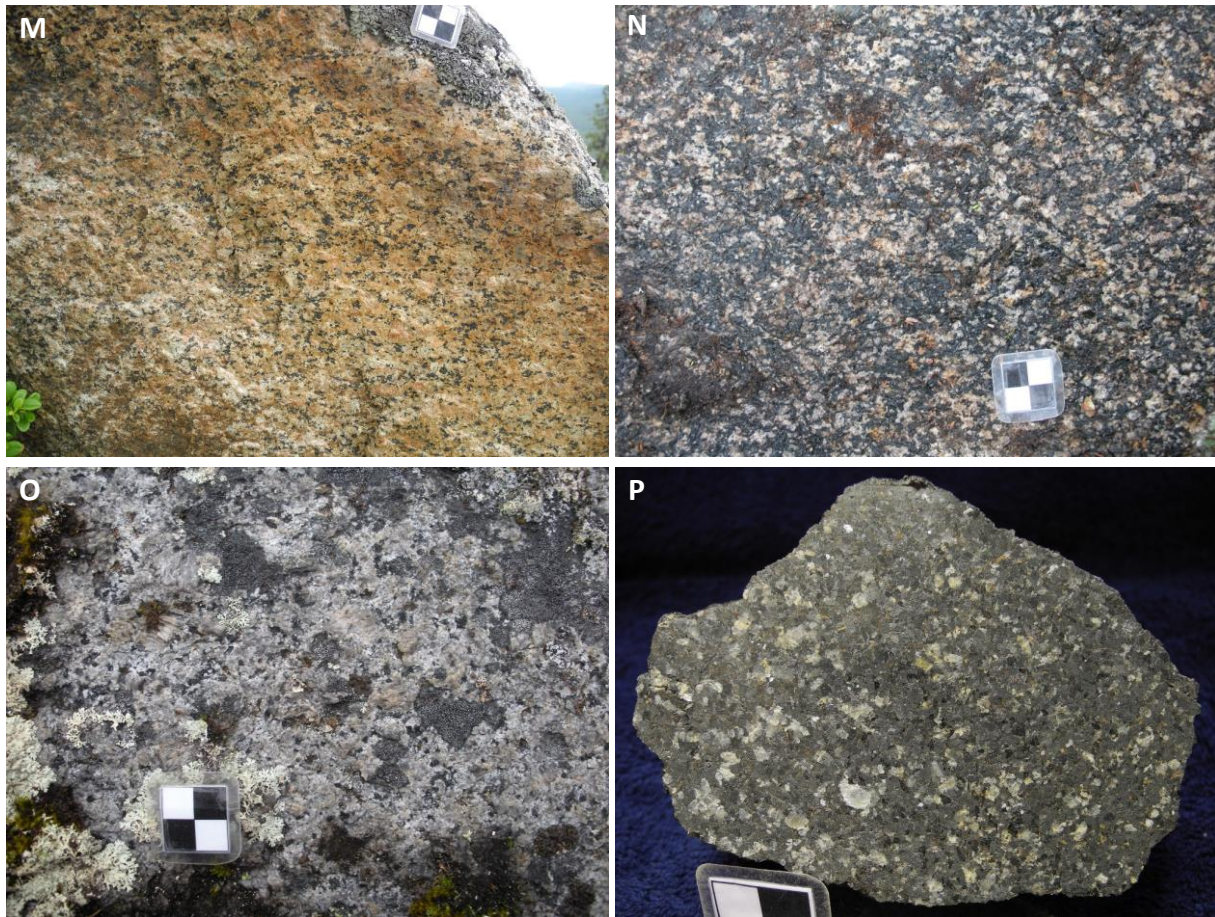


**Figure 4.** Continued. **M.** Monzodiorite that exhibits well-developed magmatic flow structures, both parallel oriented phenocrysts and dark minerals 290/8 RHR (7408199/643150). Gabbroid to dioritoid at Oarjep Gáddoajvve, **N.** magnetite-rich and biotite-bearing, **O.** plagioclase-rich (7405172/656706). **P.** Massive lamprophyric gabbroid rock from Predikstolen (7419832/636538). Photos: Dick Claeson.

### **A lamprophyric dyke associated with the Hárrevárddo intrusion**

In the coeval granite west of the circular Harrevarddo intrusion at Predikstolen (fig. 2), a narrow dyke or pipe of a black, massive, fine-grained to finely medium-grained gabbroic to ultramafic rock is found. It has high magnetic susceptibility and the plagioclase content varies between 0 and 20%. Structures and textures in the rock at the outcrop and the mineral composition studied in thin-section are interpreted as largely magmatic in origin (fig. 4P, Claeson and Antal Lundin 2015). The minerals display a subhedral, granular texture. The dominant magmatic minerals are amphibole and biotite with matrix-sized plagioclase, which indicate a kinship with lamprophyre according to IUGS terminology (Le Maitre *et al.* 2002). Lamprophyre should not contain feldspar other than in the matrix. The lamprophyric rock has a high density of  $3\,411\text{ kg/m}^3$  and a high magnetic susceptibility at  $46\,000 \times 10^{-5}$  SI units. The volume of lamprophyric rock is too small to be evident in the airborne geophysical data hence despite its high density and susceptibility it cannot be seen, either on the gravity map or the aeromagnetic anomaly map (fig. 2–3, distance between gravity stations 1 000–3 000 m and line distance 200 m). A detailed ground geophysical survey of the structure would be difficult because of the very steep topography in the area. The lamprophyric dyke is interpreted to belong to the magmatic events that created the Hárrevárddo intrusion at around 1.784 Ga ago and not a younger generation, since no chilled margin is present at the outcrop.

## XENOLITHS OF THE HÁRREVÁRDDO INTRUSION

Many xenoliths occur in the Hárrevárddo intrusion and in some places, these form more coherent areas, but is nonetheless considered to be xenoliths because they are completely enclosed by younger intrusive rocks. Most xenoliths consist of older, metamorphosed rocks from the surrounding area such as metarhyolite to metadacite, quartzite, metaarkose, metasedimentary migmatites, and paragneiss (fig. 5). Gabbro shows chilled contacts against xenoliths. Granite is often more fine-grained towards contacts with larger quartzite xenoliths as a result of faster cooling, and granite dikes appear as well in the quartzite at these occurrences. Layering in volcanic xenoliths is cut by massive monzonite to granite dikes.

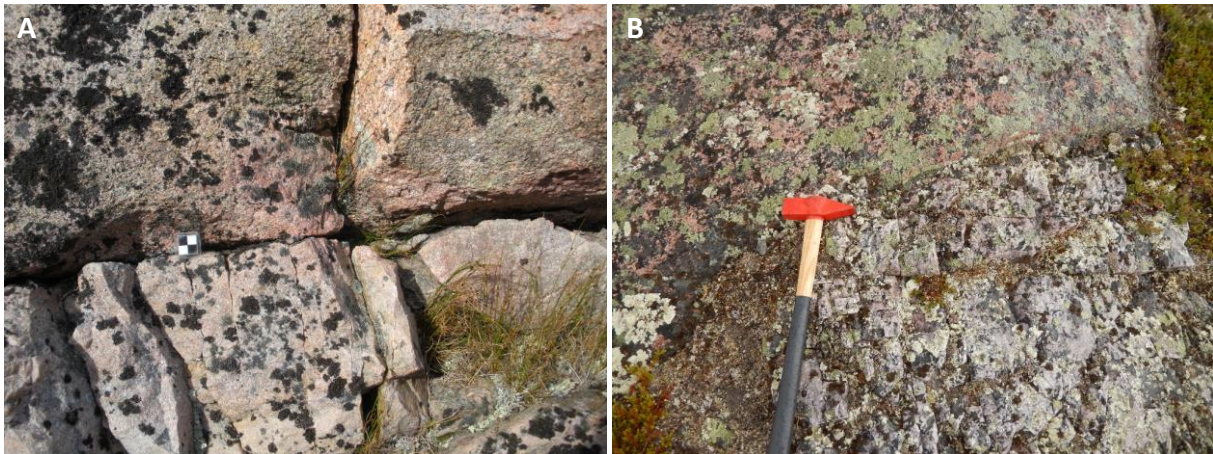


**Figure 5.** Contacts between intrusive rocks and large xenoliths of metasedimentary rocks. **A.** K-feldspar porphyritic granite to monzonite that is finer grained towards contact with quartzite (7402697/649698). Photo: Dick Claeson. **B.** Contact between medium-grained, red granite and quartzite without significant grain-size reduction (7410730/658435). Photo: Ildikó Antal Lundin.

## PETROGRAPHY OF SOME ROCKS OF THE HÁRREVÁRDDO INTRUSION

In general, the quartz monzonite, quartz monzodiorite, and monzodiorite contain potassium feldspar phenocrysts with Carlsbad twinning and inclusions of plagioclase. Plagioclase has minor sericite alteration and minor blobs of myrmekite are present. Magmatic amphibole is dark to light green, sometimes with pleochroism. Biotite is usually brownish coloured and exhibit very minor alteration to chlorite. Quartz has weakly developed undulose extinction. Accessory minerals are opaque minerals, mostly magnetite and a few sulphide mineral grains, apatite, and small zircon.

The age determined rock at Jervas is porphyritic with 10–20 mm sized phenocrysts of potassium feldspar (fig. 4B, C). The potassium feldspar shows Carlsbad twinning and phenocrysts have inclusions of plagioclase (fig. 6A, B). Plagioclase has minor sericite alteration and minor blobs of myrmekite are present. Magmatic amphibole is dark to light green pleochroic and biotite brownish coloured. Quartz shows weakly developed undulose extinction. Accessory minerals are opaque minerals, mostly magnetite and not many sulphide mineral grains, apatite, and small zircon.

The potassium feldspar porphyritic quartz monzonite to quartz monzodiorite at the Hárrevárddo mountain (fig. 4G) shows Carlsbad and tartan twinning (fig. 6C, D). Plagioclase shows minor sericite alteration and minor blobs of myrmekite are present. Quartz shows weakly developed undulose extinction. Magmatic amphibole is green and biotite shows brown to pale green pleochroism with very minor alteration to chlorite. Accessory minerals are opaque minerals, mostly magnetite and few sulphide mineral grains, apatite, and small zircon.

At Ganijvárre just north of Lillselet, an amphibole-bearing, potassium feldspar porphyritic monzodiorite to quartz monzodiorite occurs (fig. 4K). The magmatic amphibole is green and biotite brown (fig. 6E, F). Plagioclase shows minor sericite alteration and minor blobs of myrmekite are present. Potassium feldspar shows Carlsbad twinning and not much alteration. Quartz shows weakly developed undulose extinction. Accessory minerals are opaque minerals, mostly magnetite and the odd sulphide, apatite, and small zircon.

The layered gabbro at the Hárrevárddo “ring dyke” structure is in parts easily weathered (fig. 4H). Plagioclase is the most abundant mineral with minor sericite alteration (fig. 6G–J). The most abundant mafic minerals are pyroxenes. In the easily weathered variety of the gabbro both pyroxenes are present, orthopyroxene showing weak pleochroism green to pink and clinopyroxene a greenish hue (fig. 6G–J). The orthopyroxene mostly occurs as aggregates of crystals (fig. 6G, H). Clinopyroxene is both seen as solitary grains and as part of a poikilitic texture, oikocrysts with plagioclase as chadacrysts (fig. 6I, J). The other main type of gabbro at Hárrevárddo shows more resilience to weathering. Plagioclase is the most abundant mineral but less so than in the easily weathered gabbro. The most abundant mafic mineral is magmatic amphibole, almost three times as much compared with the easily weathered gabbro. Clinopyroxene occurs as grains and no oikocrystic crystals were observed, but aggregates of several individual crystals (fig. 6K, L). No orthopyroxene was observed. Amphibole has crystallised along clinopyroxene crystals but in this rock mostly in interstitial positions and not so much along rims. Almost all clinopyroxenes in both varieties have rims of magmatic amphibole, which is due to elevated H<sub>2</sub>O build-up during late-stage crystallisation. Note that these rims have the same crystallographic orientation even in the case of oikocrystic clinopyroxene (fig. 6I, J). Apart from the rims, amphibole also forms clusters with biotite and opaque minerals. Magmatic amphibole is pleochroic with dark to pale green colours in both. The biotite has dark to pale brownish pleochroism. Opaque minerals are magnetite and the odd sulphide crystal. Minor amounts of potassium feldspar and quartz are mostly found as interstitial, late-crystallising minerals along with apatite in both varieties.

The sample from Doaresoajvve is an uneven-grained to porphyritic gabbro, centrally positioned within the Hárrevárddo intrusion (fig. 4J). Plagioclase is present as matrix and phenocrysts up to 20 mm in length showing minor sericite alteration (fig. 6M, N). The most abundant mafic mineral is magmatic amphibole that is green, the clinopyroxene shows a weak greenish tint, and biotite a brownish. Minor amounts of apatite and opaque minerals, mostly magnetite and the odd sulphide crystal are also present. Potassium feldspar and quartz are mostly found as interstitial, late-crystallising minerals.

The gabbro from Oarjep Gáddoajvve is iron-rich, where the mafic minerals mostly are magmatic amphibole, biotite, and magnetite (fig. 4N). Amphibole is green and euhedral crystals are not uncommon (fig. 6O–V). Plagioclase is fresh and only minor sericite alteration is seen (fig. 6O–R). Brown biotite is mostly not altered, but in places severely altered to chlorite (fig. 6S, T). Poikilitic biotite shows chadacrysts of plagioclase and magnetite (fig. 6U, V). Interstitial, poikilitic and late-forming olivine occur (fig. 6O, P, S, T). The oikocrysts of olivine have chadacrysts of plagioclase and amphibole (fig. 6O, P, S, T). Quartz occurs interstitially, showing feeble undulose extinction (fig. 6Q, R). Opaque minerals are magnetite and some apatite are present as well. The crystallisation order would then be plagioclase+amphibole+magnetite+apatite, and later interstitially biotite, olivine, and quartz. Since there is quartz present in the thin-section the composition of olivine has to be fayalitic, in accordance with the iron-rich nature of the gabbro.

The lamprophyric gabbroic rock at Predikstolen is massive and has a subhedral, granular texture (fig. 4P). The mineral distribution is plagioclase 15%, amphibole 38%, biotite 24%, apatite 0.5%, 4% clinopyroxene (severely altered, probably hydrothermally during late- or post-magmatic cooling), and 18% opaque minerals. Amphibole is present as subhedral to euhedral, pleochroic dark to light green crystals (fig. 6W, X). Biotite is subhedral and shows pleochroism from dark

reddish brown to pale brown. Plagioclase is subhedral, showing minor sericite alteration, and no phenocrysts are present. Most of the opaque minerals are magnetite and some sulphide minerals occur. There are also small crystals of olivine and zircon, possibly rutile.

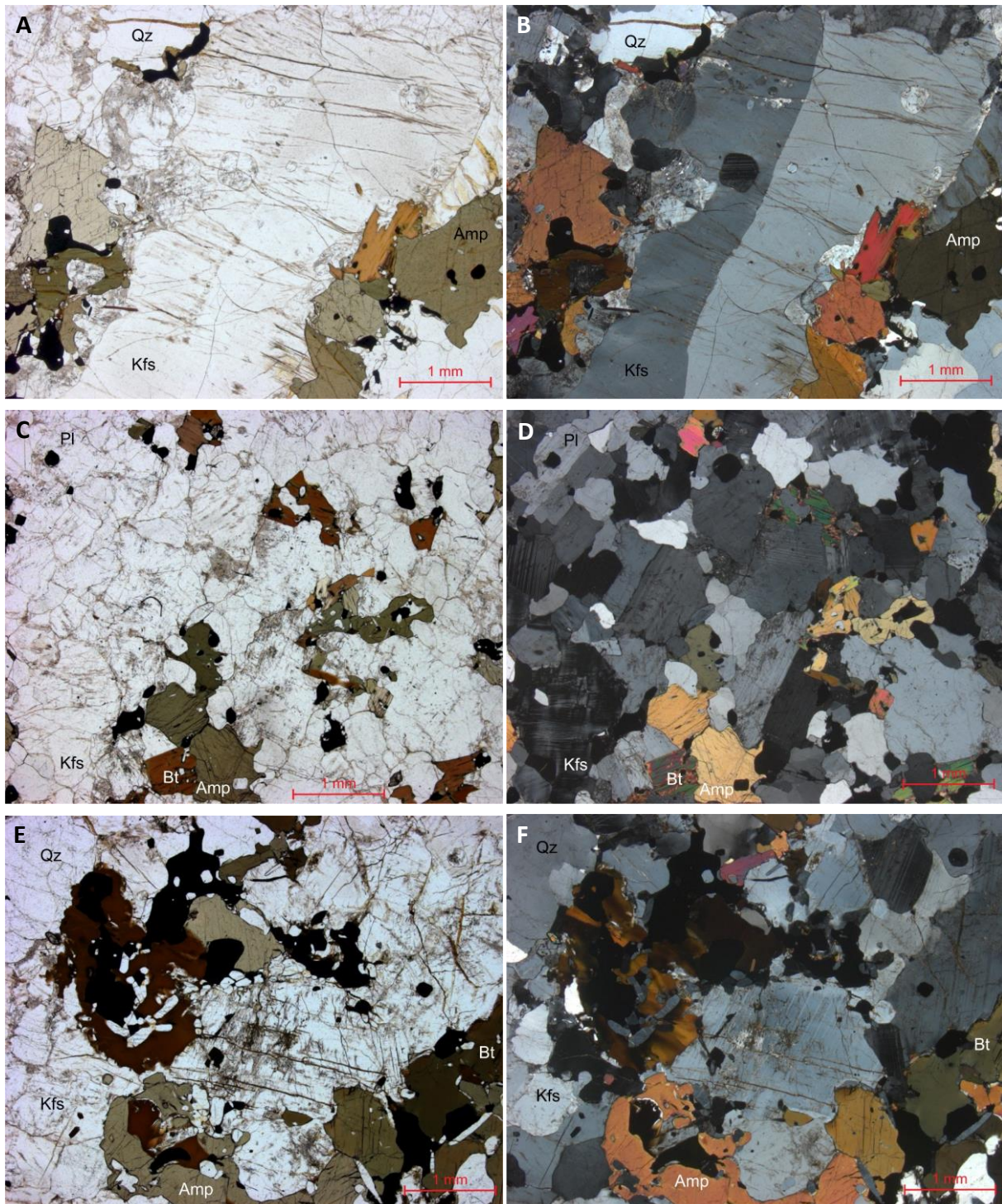


**Figure 6.** The age determined quartz monzonite at Jervas shows potassium feldspar phenocrysts with inclusions of plagioclase, magmatic amphibole and biotite, **A.** plane-polarized light and **B.** crossed nicols (7403249/650222). Potassium feldspar porphyritic quartz monzonite to quartz monzodiorite from Hårrevårddo, with potassium feldspar showing Carlsbad and tartan twinning, **C.** plane-polarized light and **D.** crossed nicols (7414364/656970). At Ganijvärre just north of Lillelet magmatic amphibole is green and biotite dark brown, plagioclase shows minor sericite alteration in K-eldspar porphyritic monzodiorite to quartz monzodiorite, **E.** plane-polarized light. and **F.** crossed nicols (7408249/643510).

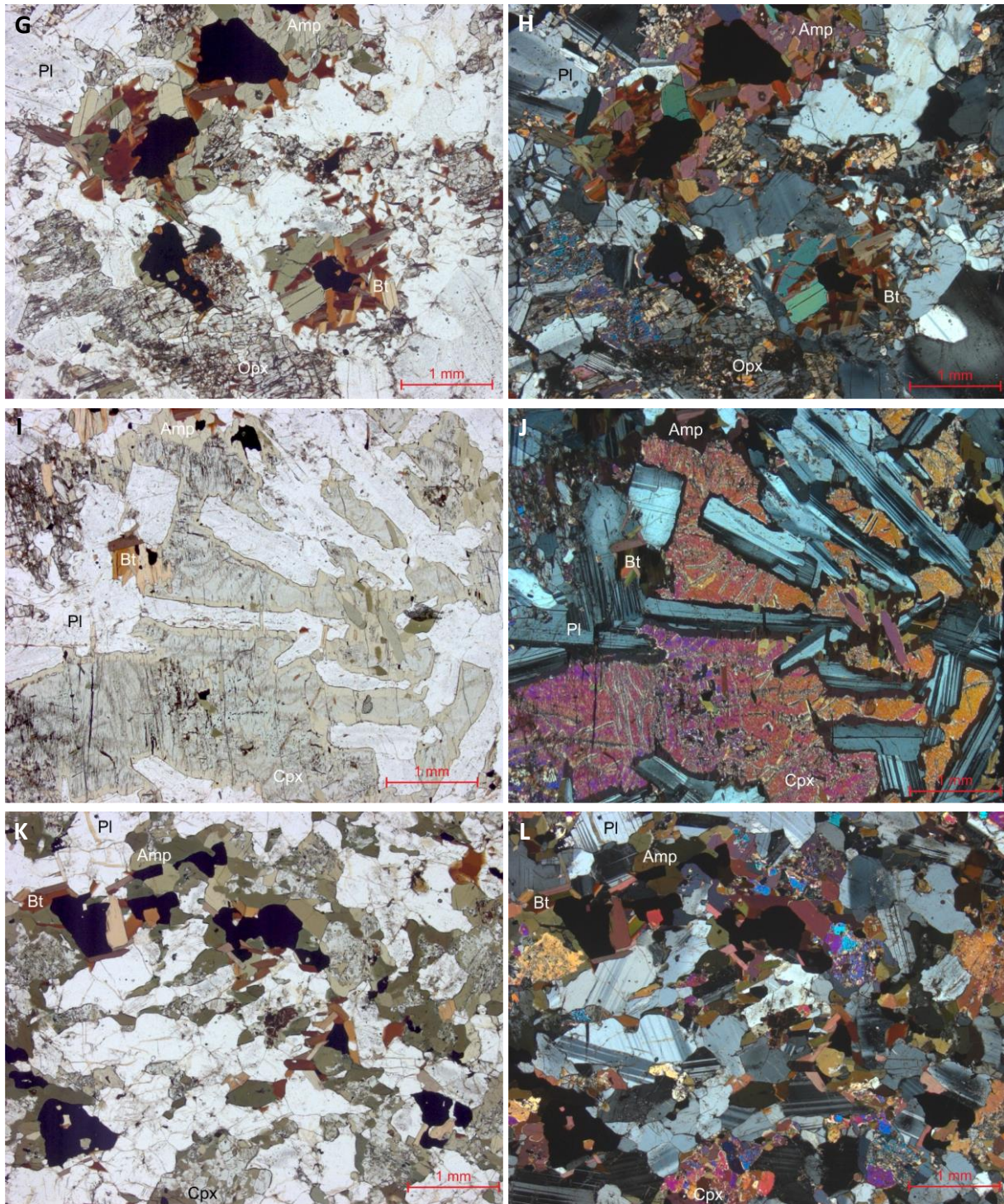


**Figure 6.** Continued. Orthopyroxene as aggregates of crystals in easily weathered gabbro at the Hárrevárddo mountain. Clusters of magmatic amphibole, biotite, and opaque minerals, **G**, plane-polarized light and **H**, crossed nicols (7414486/657886). Easily weathered gabbro at Hárrevárddo shows poikilitic clinopyroxene with plagioclase as chadacrysts, rims of magmatic amphibole on their perimeter. Note that the rims have the same crystallographic orientation, **I**, plane-polarized light and **J**, crossed nicols (7414486/657886). Resilient gabbro at Hárrevárddo with plagioclase showing minor sericite alteration and amphibole crystallized in interstitial positions, **K**, plane-polarized light and **L**, crossed nicols (7414486/657886).

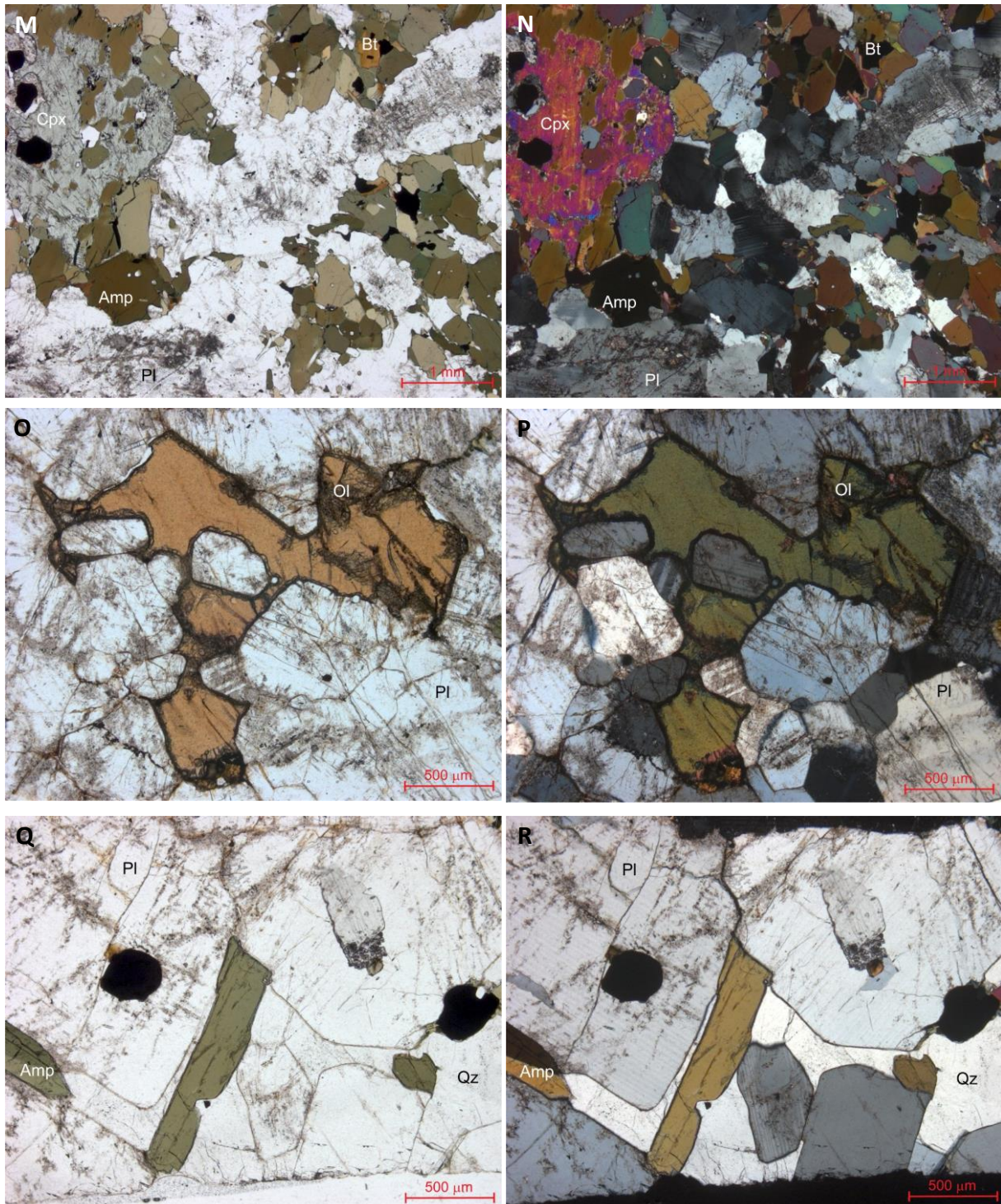


**Figure 6.** Continued. An uneven-grained to porphyritic gabbro from Doaresoajvve, centrally positioned within the Hárrevárddo intrusion, with plagioclase present as matrix and up to 20 mm large phenocrysts showing minor sericitic alteration, **M.** plane-polarized light and **N.** crossed nicols (7412949/645879). Interstitial olivine in iron-rich gabbro from Oarjep Gáddoajvve that possibly shows chadacrysts of plagioclase, **O.** plane-polarized light and **P.** crossed nicols (7405172/656706). Interstitial quartz in iron-rich gabbro from Oarjep Gáddoajvve showing feeble undulose extinction, **Q.** plane-polarized light and **R.** crossed nicols (7405172/656706).

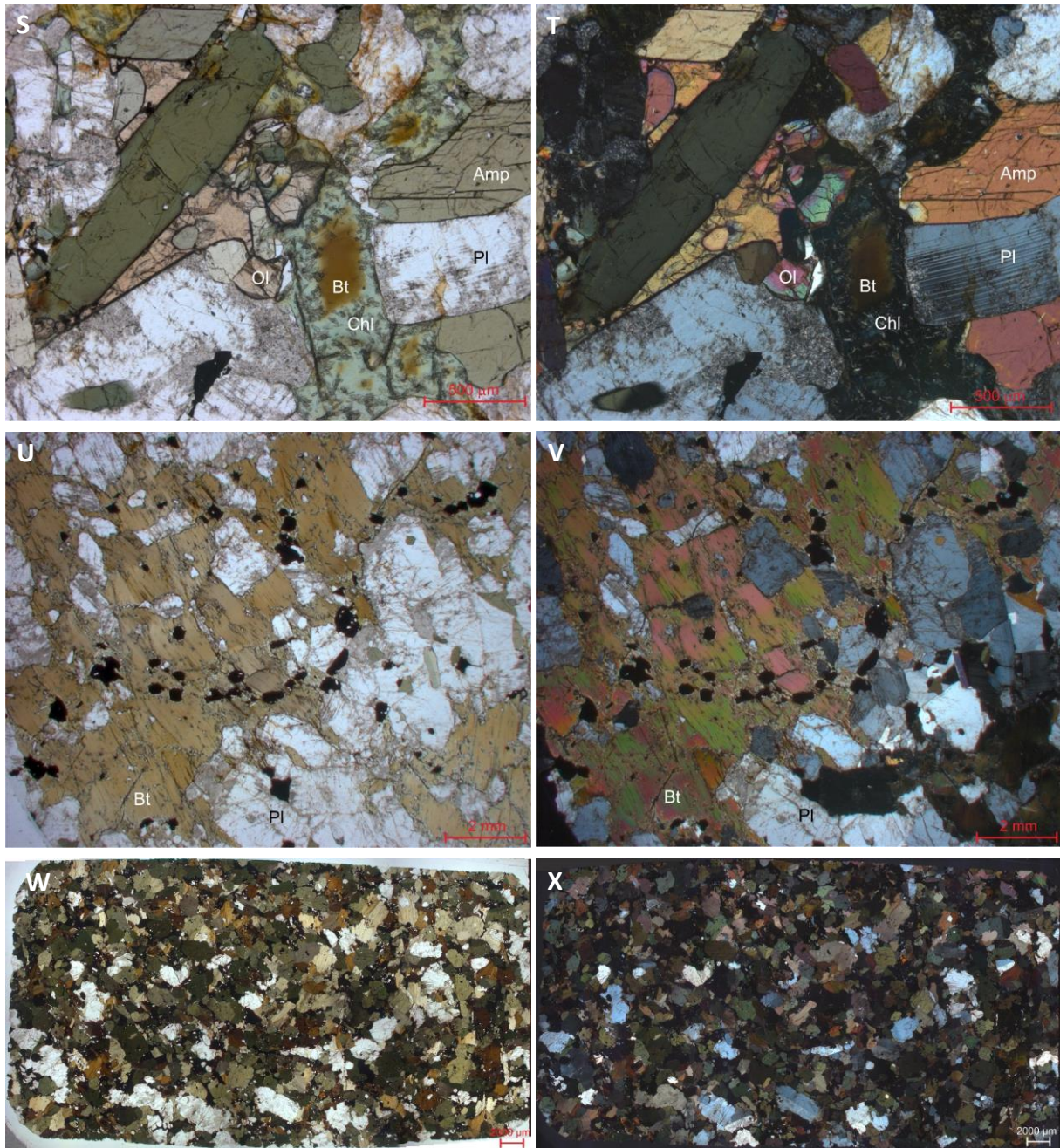


**Figure 6.** Continued. Interstitial, late-forming olivine in iron-rich gabbro from Oarjep Gáddoajvve with amphibole as chadacryst. Biotite severely altered to chlorite, **S.** plane-polarized light and **T.** crossed nicols (7405172/656706). Poikilitic biotite shows chadacrysts of plagioclase and magnetite in iron-rich gabbro from Oarjep Gáddoajvve, **U.** plane-polarized light and **V.** crossed nicols (7405172/656706). Full thin-section, showing amphibole, biotite, plagioclase, and opaque minerals as subhedral, granular textured lamprophyric gabbroid, **W.** plane-polarized light and **X.** crossed nicols (7419832/636538). Photos: Dick Claeson. All mineral abbreviations according to Whitney & Evans (2010).

## **INTERNAL CONTACTS AND MAGMATIC FLOW RELATED STRUCTURAL ELEMENTS OF THE HÁRREVÁRDDO INTRUSION**

Almost all contacts within the Hárrevárddo intrusion are sharp and not gradational. This is also true between the acid rocks of different compositions and for the most part also for rocks of all compositions whether porphyritic or not. Even though contacts are sharp, most are winding and wavy in appearance, not straight for long distances (fig. 4I). Chilled margins are not observed among the interpreted coeval rocks within the Hárrevárddo intrusion.

The measurements of contacts between basic rocks of the Hárrevárddo “ring dyke” structure and acidic rocks show plunges from 60 to 80 degrees. The 2.5 modelling indicate that the contacts may even have steeper dip at depth (fig. 13). The few measurements of layering within the basic rocks of the “ring dyke” structure have a plunge around 65 degrees. Magmatic foliation in adjacent monzodiorite to quartz monzodiorite strikes along the contact at 20/80 (RHR), away from the contact.

Magmatic foliations and lineations are indicated by the preferred orientations of potassium feldspar phenocrysts and mafic minerals. Microstructures are either magmatic features or formed during early solid-state deformation, near solidus conditions. Magmatic flow structures seen as foliation along the western contacts at several outcrops may also be related to a magmatic deformation zone that is only present inside the Hárrevárddo intrusion (fig. 2, 9), with moderate dip around 50 to more steep at 80 degrees and all towards east, but still located within the 1.78–1.79 Ga intrusion.

## **CONTACTS WITH THE SURROUNDING ROCKS AND INTRUSION RELATED METAMORPHISM**

Contacts with the older, surrounding rocks are only observed at few locations due to the quaternary cover or very steep topography. Contact metamorphism occurs at the margins of the Hárrevárddo intrusion, which is evidence of a thermal contrast between the magma and its host rocks, and the contacts with the surrounding rocks are sharp. An example can be studied c. 3 km south of the Hárrevárddo mountain, just east of Jiervavárddo, where metaarkose are very heterolithic with abundant clasts of sedimentary and volcanic rocks, with metre-long streaks of sillimanite in the plane of foliation in the metaarkose and incipient partial melting seen as leucosomes in migmatitic parts (Claeson & Antal Lundin 2019). Just several tens of meters further to the east, a dacitic metavolcanic rock also has veins. At Njallatjåhkkå, c. 4 km east of Jervas, a diatexitic granite occurs that formed from melting of banded dacite to rhyolite. Garnet and sillimanite ± andalusite with anatexis but lack of cordierite in most metasedimentary rocks of the c. 1.87–1.84 Ga Snavva-Sjöfallet Group north of the Hárrevárddo intrusion, points to a metamorphic pressure above 3 kbar for the surrounding rocks (Claeson and Antal Lundin 2015). The indicated temperature is above 650–700 °C, where partial melting under water-saturated conditions starts in pelitic rocks (Bucher & Frey 1994). Most of the rocks encountered are metaarkose or at least show lower amounts of clay minerals than ordinary pelite. The quartzite of Snavva-Sjöfallet Group does not contain any aluminium silicates due to its silica-rich composition. Most observations are that in connection with intrusion of the large syenitoid to granitic plutons within the study area, the magmatism caused metamorphism and deformation. The intrusions are obviously younger than the sedimentary rocks of the Snavva-Sjöfallet Group. The metasedimentary rocks are aligned outside the intrusion and have been compressed and folded in the areas where they were deformed in connection with the magmatic activity, having different directions of fold axis than measured in the region. An example is seen north of Njavve, c. 17 km

northwest of Hárrevárddo, where there is a conglomerate belonging to the Snavva-Sjöfallet Group (Claeson & Antal Lundin 2019). A large heterogeneity is seen within the conglomerate regarding how well-preserved different parts of the conglomerate is (fig. 7). The changes are gradational and take place over a few meters and result in a rock that is almost no longer being recognizable as belonging to the conglomerate and instead viewed as a strongly deformed and migmatized gneiss (Claeson & Antal Lundin 2019). The above explains why the Snavva-Sjöfallet Group sedimentary rocks may have very well-preserved structures, such as ripple marks, in other places where heat and deformation generated by the magmatic activity of around 1.80 Ga ago has not occurred or been so extensive. An alternative explanation would be a strain localisation older than the Hárrevárddo intrusion within the conglomerate that also generated melting, however, such an event would possibly occur at greater depth than the estimate of above 3 kbar from the metamorphic index minerals present.

The distribution of supracrustal rocks limit the Hárrevárddo intrusion margins in the N, E and S, but the position of the W contact is unclear (fig. 1–3). As stated above the rocks outside the near circular, central part of the anomaly that are interpreted to be of more or less coeval magmatism continue in the west. There are also rocks interpreted as coeval, but formed prior to the circular intrusion, beyond the enveloping supracrustal rocks to the east and south (Claeson & Antal Lundin 2019). A coeval  $9.5 \times 6.5$  km large satellite intrusion is also present in older supracrustal rocks just north of Tjåmotis, 6 km north of the Hárrevárddo intrusion (southern part seen in fig. 1). However, this satellite intrusion does not display the diversity of rock types as the Hárrevárddo intrusion (Nysten *et al.* 2014).

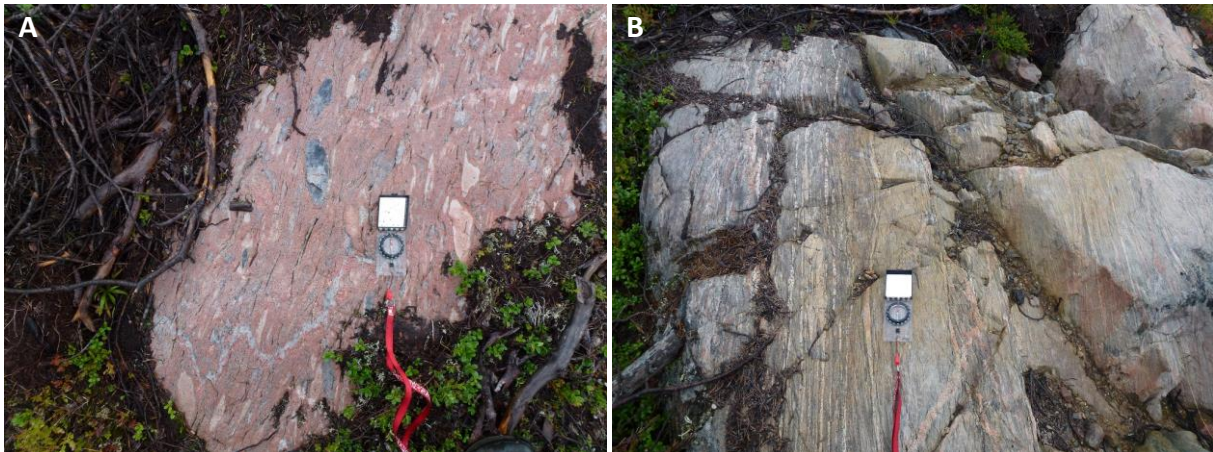


**Figure 7.** A. Well-preserved conglomerate, belonging to the Snavva-Sjöfallet Group (7423459/641991). B. Same conglomerate as in A. transformed into strongly deformed and migmatized gneiss (7423986/642116). Photos: Charlotta Brandt.

## STRUCTURAL ELEMENTS WITHIN AND IN SURROUNDING ROCKS OF THE HÁRREVÁRDDO INTRUSION

The surrounding rocks are foliated, at places lineated and folded (Claeson & Antal Lundin 2019). The regional deformation is regarded to have occurred prior to the formation of the Hárrevárddo intrusion at c. 1.88–1.87 Ga (Claeson & Antal Lundin 2019). The regional direction of foliation of the surrounding area is north-northeast to south-southwest and (Claeson & Antal Lundin 2019, fig. 8A). Close to the Hárrevárddo intrusion, foliation is seen conformable with the perimeter of the younger rocks and thus formed in a ductile manner at around 1.80 Ga ago (fig. 8B, 9). The fold axis, tectonic foliation and layering seen inside the Hárrevárddo intrusion in figure 9 are for the most part that of larger areas of xenolithic rocks. From figure 9 it is evident that the Hárrevárddo intrusion is a discordant pluton.

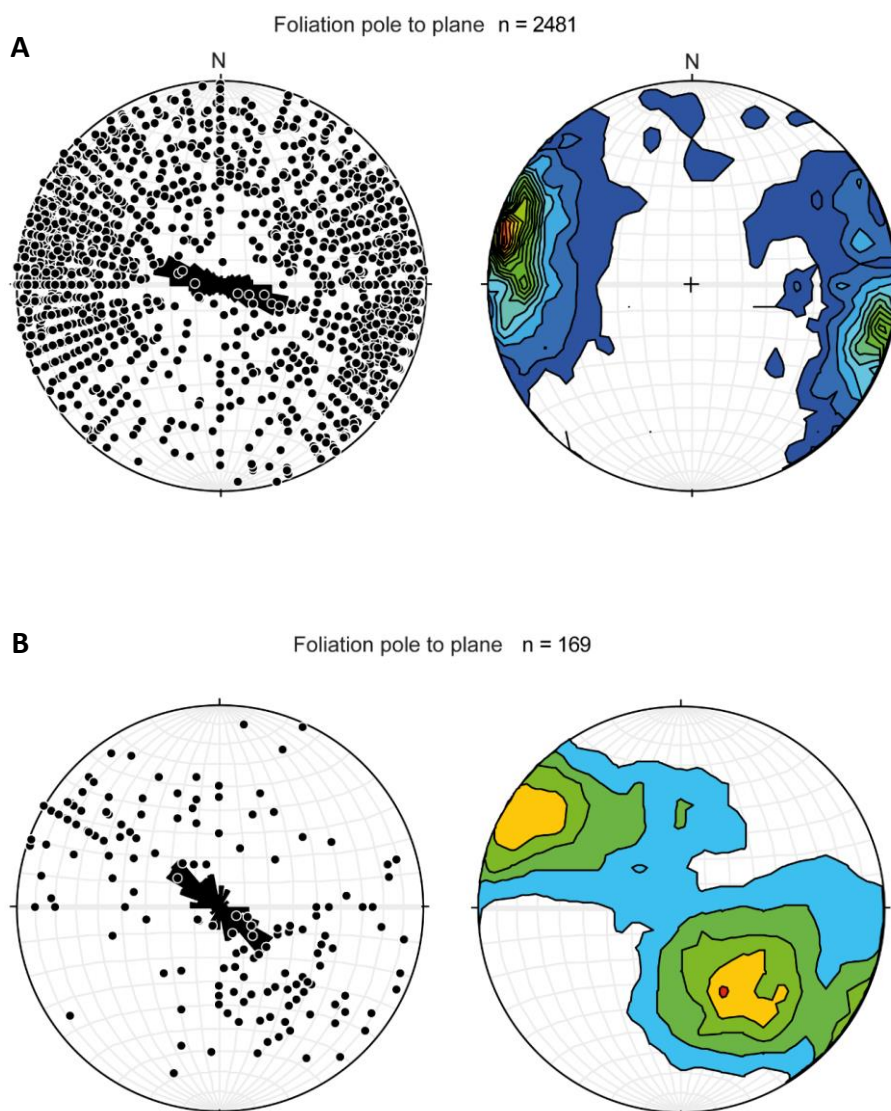


**Figure 8. A.** Foliation measurements from map areas 27I Tjåmotis SV, SO, 26J Jokkmokk NV, NO, and 26I Porjus SV. **B.** Foliation measurements from map area Tjåmotis SV. All foliations plotted in Schmidt net, lower hemisphere.

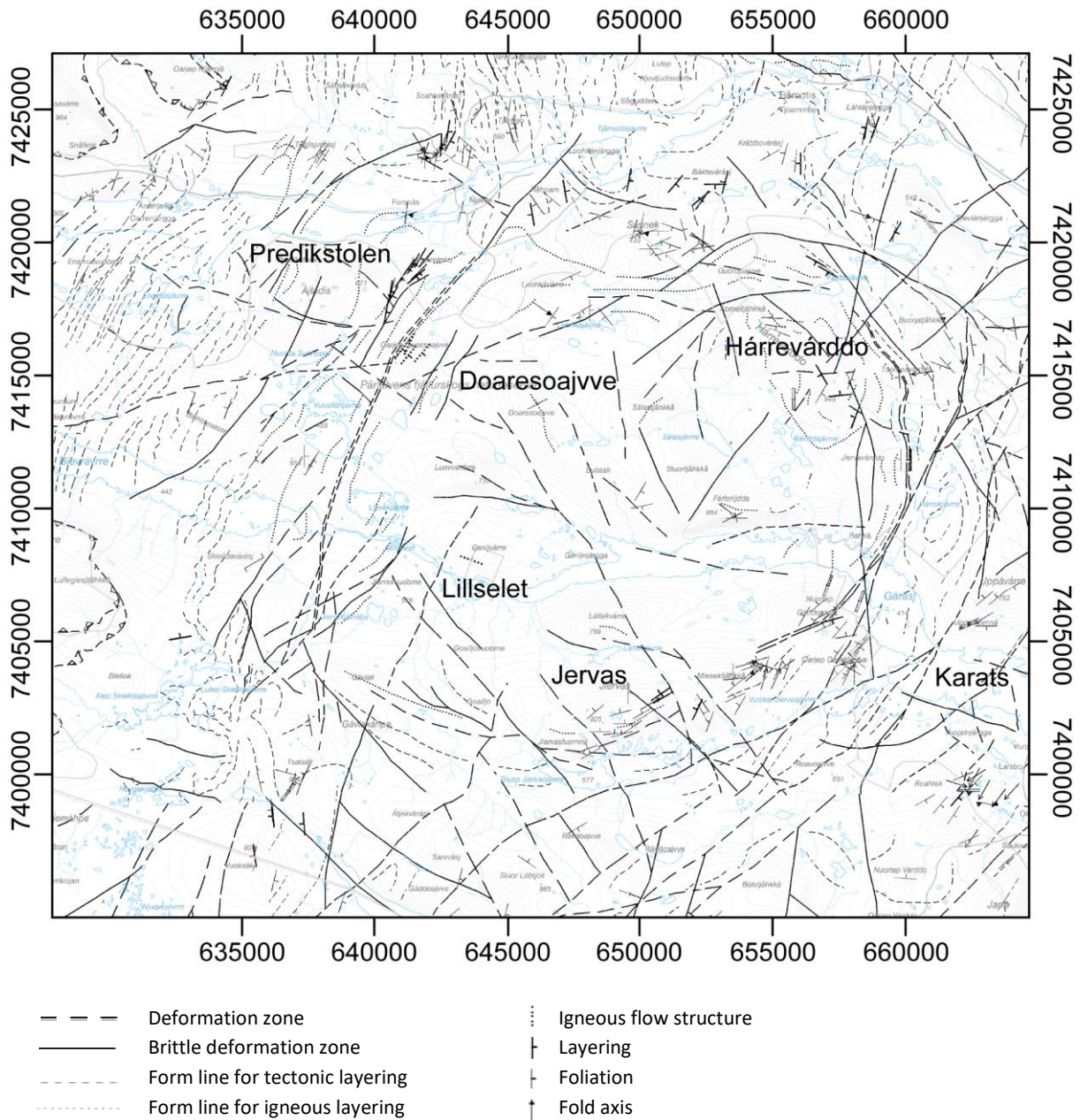


**Figure 9.** Structural elements in the study area of the Hárrevárddo intrusion.

At several large slab-like outcrops, exfoliation and banking is seen over long distances (fig. 10A, B). Some correspond to the measured flow foliation and at other outcrops the granite to monzodiorite rocks look massive yet display banking. At some outcrops it is evident that banking follows an internal structure seen in the rock (fig. 10C).

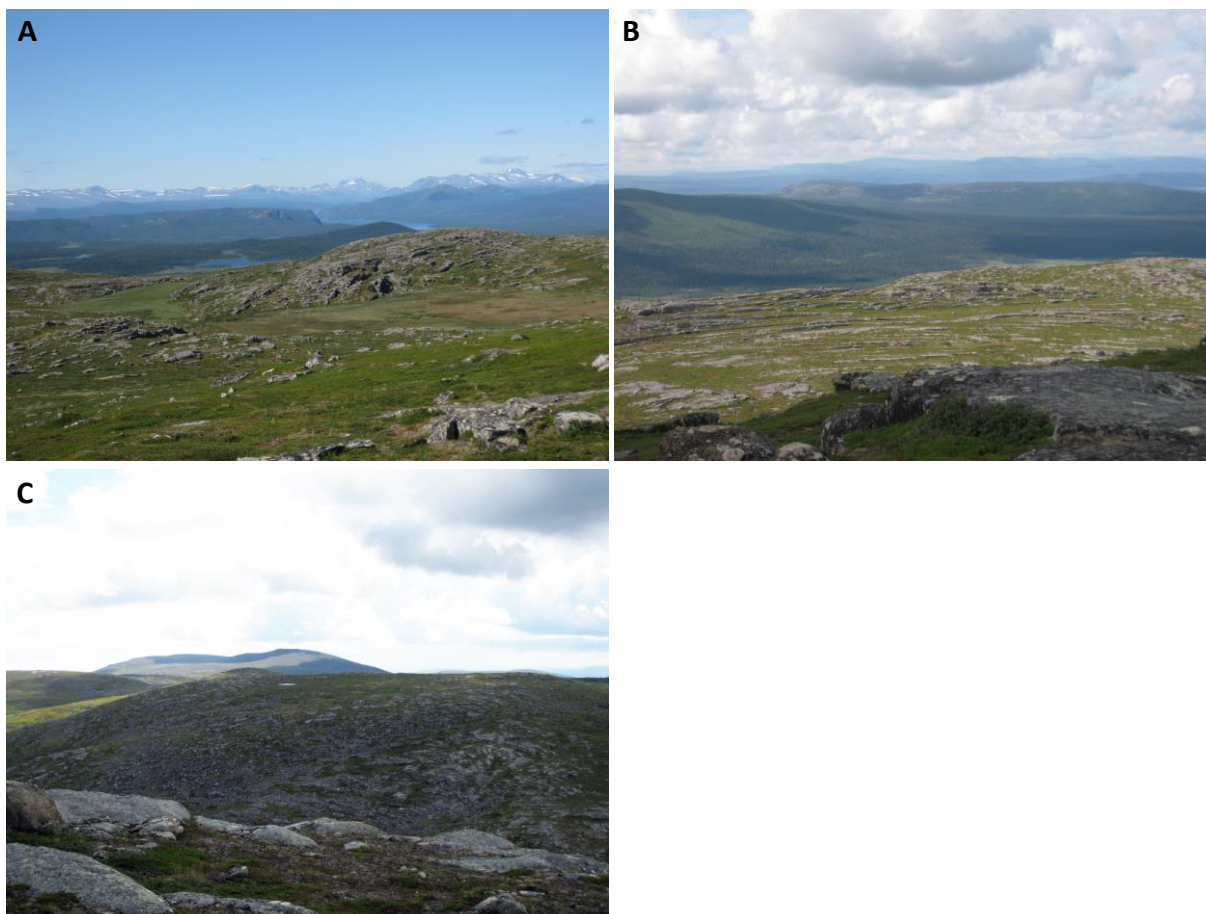


**Figure 10.** Outcrops showing exfoliation and banking at Hárvárddo summit. **A.** Hill with monzodiorite and granite to monzonite towards the photographer. **B.** Slab-like outcrop of granite to monzonite. **C.** Banking following internal magmatic structure in granite. Photos: Ildikó Antal Lundin.

## WHOLE-ROCK GEOCHEMISTRY OF ROCKS FROM THE HÁRVÁRDDO INTRUSION

The rocks classified in outcrops as gabbro, monzodiorite, quartz monzodiorite, and quartz monzonite of the Hárvárddo intrusion, exhibit a fractionation trend in the REE diagram entirely consistent with their petrographic classification (fig. 6A, Table 1). The gabbro at the Hárvárddo mountain displays the lowest levels of REE, which then increase systematically to the quartz monzonite. The magnetite-rich gabbro at Oarjep Gáddoajvve (fig. 4N, 6O–V), is interpreted to be coeval with the Hárvárddo intrusion but intruded in surrounding volcanic rocks to the southeast (fig. 1, 2). It has significantly higher levels of REE than the gabbro at Hárvárddo and has higher levels of HREE than the more acidic rocks (fig. 11A). This is probably due to fractionation in a magma chamber of basic composition at greater depths than the Hárvárddo intrusion. This deduction is most clearly seen in the significant Eu anomaly of the magnetite-rich gabbro ( $\text{Eu}/\text{Eu}^* = 0.24$ ), indicating that significant amounts of plagioclase-rich basic magma fractionated before the magnetite-rich gabbro magma formed and ascended (fig. 11A). Even in the multi-element diagram, the rocks of the Hárvárddo intrusion show similar profiles, while the magnetite-rich gabbro differ somewhat, especially with its deep Zr anomaly but show the same trough for Sr and P, as well as for Eu and Ti like the acid rocks do (fig. 11B). All samples display flat HREE patterns, which is indicative of no major presence of garnet residues at their region of melt generation.

The age determined quartz monzonite from the Hárrevárdó intrusion, Jervas, was shown to have more or less identical patterns in the REE and multielement diagrams with an 100 Ma older, age determined metamorphic monzonite at Njuorramjauratj, some 44 km NE of Jervas (Claeson *et al.* 2018c, Claeson & Antal Lundin 2019). The reasons advocated was that the same magmatic processes, degree of melting, magmas generated from the same or very similar source material, and formed during similar pressure and temperature conditions, generate exactly the same magma compositions, regardless of what geological period this occurs in.

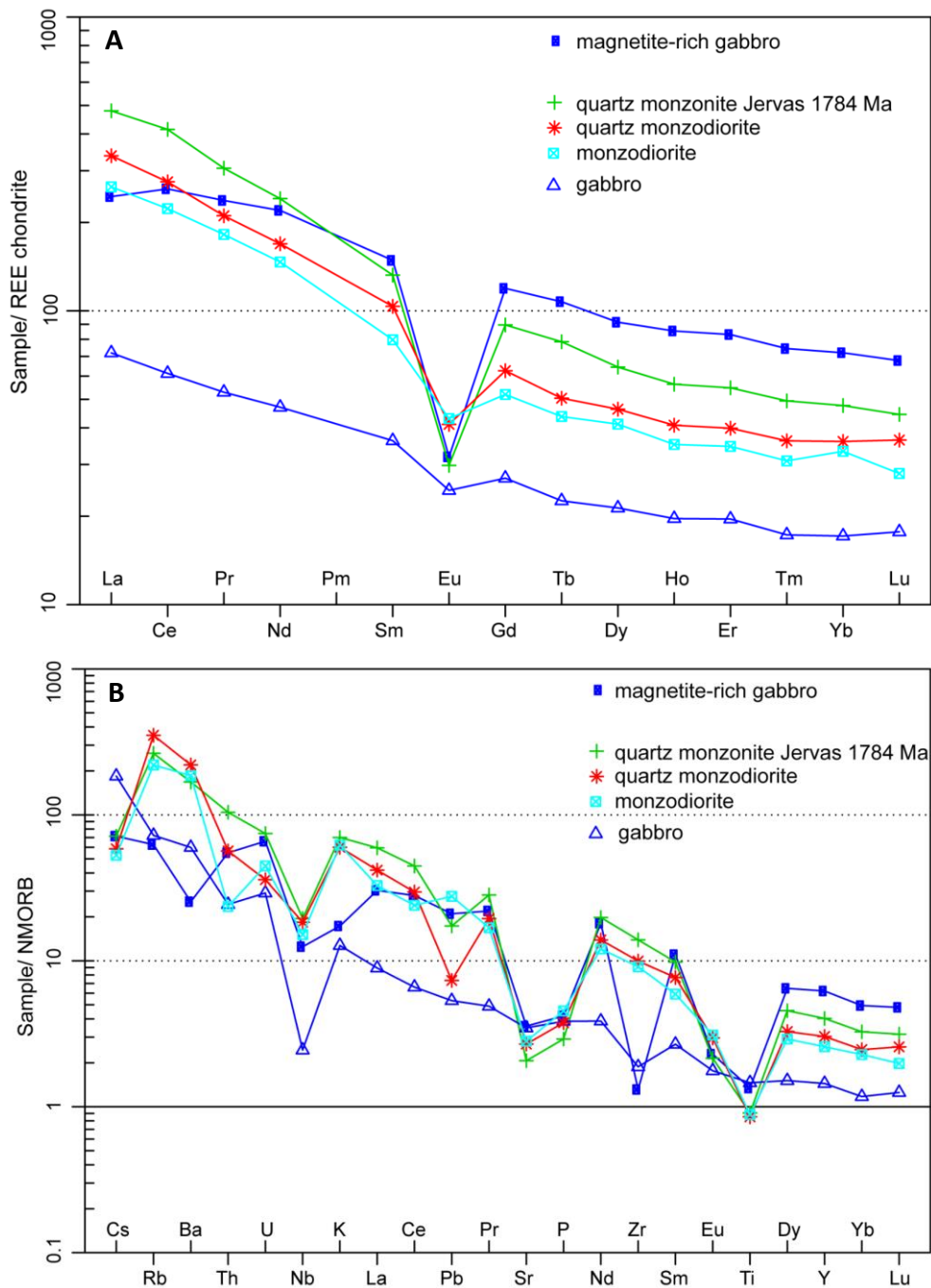


**Figure 11.** A. REE diagram of coeval rocks from the Hárrevárdó intrusion. Normalizing values for chondrite from Boynton (1984). B. Spider diagram of rocks as in A. Normalizing values for N-MORB from Sun & McDonough (1989).

**Table 1.** Whole-rock geochemistry of rocks from the Hárrevárddo intrusion. Oxides (wt %) and trace elements (ppm). A = Magnetite-rich gabbro, Oarjep Gáddoajvve, B = Quartz monzonite, Jervas, C = Gabbro, Hárrevárddo, D = Quartz monzodiorite Hárrevárddo, E = Monzodiorite, Ganijvárre N of Lillelet.

	A	B	C	D	E		A	B	C	D	E
<b>SiO<sub>2</sub></b>	47.42	62.58	48.2	65.7	64.1	<b>Tm</b>	2.41	1.60	0.56	1.17	1.00
<b>Al<sub>2</sub>O<sub>3</sub></b>	14.56	14.25	15.2	13.85	14.4	<b>U</b>	3.10	3.50	1.37	1.69	2.10
<b>Fe<sub>2</sub>O<sub>3</sub></b>	18.54	8.18	14.35	6.69	7.07	<b>V</b>	302	52	351	38	55
<b>CaO</b>	5.95	2.92	7.78	2.6	3.3	<b>Y</b>	174	113	40.4	84.8	72.1
<b>MgO</b>	4.21	1.22	5.92	1.03	1.21	<b>Yb</b>	15.0	9.95	3.58	7.51	6.95
<b>Na<sub>2</sub>O</b>	4.39	3.34	2.78	3.38	3.67	<b>Zr</b>	97.1	1030	139	737	674
<b>K<sub>2</sub>O</b>	1.25	5.06	0.92	4.33	4.49	<b>Bi</b>	0.05	0.05	0.02	0.01	0.01
<b>TiO<sub>2</sub></b>	1.7	1.15	1.85	1.08	1.12	<b>Hg</b>	0.02	0.005	0.016	0.011	0.009
<b>MnO</b>	0.26	0.12	0.19	0.13	0.1	<b>Sb</b>	0.1	0.05	0.19	0.025	0.05
<b>P<sub>2</sub>O<sub>5</sub></b>	0.49	0.34	0.45	0.44	0.53	<b>Se</b>	0.25	0.25	0.8	2.3	0.9
<b>LOI</b>	0.9	0.4	0.2	0.79	0.5	<b>Te</b>	n/a	n/a	0.005	0.01	0.01
<b>Sum</b>	99.69	99.6	97.9	100	100.7	<b>Ag</b>	0.05	0.05	0.02	0.03	0.04
<b>C</b>	0.04	0.02	0.02	0.01	0.01	<b>As</b>	3.4	1.2	3.3	1.4	0.3
<b>Ba</b>	160	1059	377	1385	1170	<b>B</b>	n/a	n/a	<10	<10	<10
<b>Ce</b>	210	335	49.5	222	180	<b>Be</b>	5	2	0.15	0.37	0.5
<b>Cr</b>	82.1	144	190	170	20	<b>Cd</b>	0.1	0.05	0.04	0.03	0.09
<b>Cs</b>	0.5	0.5	1.29	0.41	0.37	<b>Co</b>	28.1	8.7	32.7	5.9	6.4
<b>Dy</b>	29.4	20.7	6.87	14.9	13.2	<b>Cu</b>	37.3	15.4	35.8	10.8	10.1
<b>Er</b>	17.4	11.5	4.11	8.37	7.26	<b>Ge</b>	n/a	n/a	0.2	0.35	0.17
<b>Eu</b>	2.34	2.19	1.80	3.02	3.16	<b>In</b>	n/a	n/a	0.017	0.04	0.041
<b>Ga</b>	36.4	23.9	23.2	27.4	24.7	<b>Li</b>	n/a	n/a	21.4	14.6	9
<b>Gd</b>	30.9	23.2	6.98	16.2	13.4	<b>Mo</b>	1.4	4.1	0.82	2.75	2.13
<b>Hf</b>	3.50	26.9	4.30	19.2	15.5	<b>Ni</b>	9.1	3.4	50.7	2.1	1.4
<b>Ho</b>	6.13	4.04	1.41	2.93	2.52	<b>Pb</b>	6.3	5.2	1.6	2.2	8.3
<b>La</b>	75.9	149	22.3	104	81.9	<b>Tl</b>	0.05	0.1	0.001	0.001	0.0005
<b>Lu</b>	2.18	1.43	0.57	1.17	0.90	<b>S</b>	0.01	0.01	0.03	0.01	0.06
<b>Nb</b>	29.1	45.4	5.7	42.8	35.2	<b>Sc</b>	46	19	4.9	4.9	5.4
<b>Nd</b>	132	144	28.2	102	88	<b>Sn</b>	9	2	0.6	1.8	0.8
<b>Pr</b>	29.0	37.3	6.45	25.7	22.2	<b>Tl</b>	n/a	n/a	0.2	0.1	0.05
<b>Rb</b>	35	148	40.5	196	123	<b>W</b>	1.6	0.25	0.17	0.23	0.08
<b>Sm</b>	29.0	25.8	7.05	20.2	15.6	<b>Zn</b>	207	79	51	49	85
<b>Sr</b>	321	186	312	242	253	<b>Au</b>	2.2	1.6	0.001	0.001	0.0005
<b>Ta</b>	1.2	1.6	0.3	1.8	2.3	<b>Pt</b>	n/a	n/a	<0.005	<0.005	0.0025
<b>Tb</b>	5.09	3.72	1.07	2.39	2.07	<b>Pd</b>	n/a	n/a	0.001	0.0005	0.001
<b>Th</b>	6.60	12.5	2.92	6.79	2.83						

## PETROPHYSICS OF ROCKS FROM THE HÁRREVÁRDDO INTRUSION

A statistical summary of the petrophysical samples from different rock types of the Hárrevárddo intrusion is given in Table 2. Density and magnetic susceptibility were used for the characterization of the physical properties of different rock types in the area and to support the interpretation of the geophysical data.

A plot of magnetic susceptibilities versus densities for gabbro-diorite samples from different places within the Hárrevárddo “ring dyke” structure shows that the magnetic susceptibilities plot in the ferromagnetic field. The density values clearly show lower densities for the porphyritic gabbro-diorite, while the even-grained gabbros from the same area have considerably higher densities suggesting a different composition (fig. 12A). All the samples except one display a Königsberger ratio  $Q$  (the ratio between remanent- and induced magnetisation) of less than 1, which means that the source of the magnetic anomalies is due to the high magnetic susceptibilities only (fig. 12B). There is only one sample each from the small plug-like intrusions Oarjep Gáddoajvve and Doaresoajvve, and their densities of about  $2\,900\text{ kg/m}^3$  differ from those of the Hárrevárddo “ring dyke” rocks  $3\,000\text{--}3\,100\text{ kg/m}^3$  (fig. 12A). The gabbroid to ultramafic rock of lamprophyric affinity from Predikstolen has a much higher density and susceptibility compared with the other samples (fig. 12A). The samples from Oarjep Gáddoajvve and Doaresoajvve show  $Q$ -values  $> 1$ , which may affect the size and shape of the magnetic anomalies (fig. 12B).

**Table 2.** Petrophysical properties of rocks from the Hárrevárddo intrusion

Rock type	N	Density ( $\text{kg/m}^3$ )			Magnetic susceptibility ( $10^{-5}$ SI)			N	Q-value		
		Mean	Min	Max	Log. Mean	Min	Max		Mean	Min	Max
Granite, porphyritic	26	2640	2537	2707	524	21	8950	21	0.8	0.1	3
Granite	32	2620	2547	2697	687	5	4100	28	0.6	0	0.9
Syenitoid	14	2625	2589	2682	890	32	4000	13	0.5	0	2.5
Monzodiorite - Quartz monzodiorite, porphyritic	10	2706	2671	2742	4153	2458	6780	10	0.3	0	0.8
Gabbro - dioritoid, porphyritic	6	2777	2701	2951	5517	2000	19800	6	4.2	0.6	16.7
Gabbro - dioritoid	40	3041	2766	3411	7519	147	45600	40	2.5	0.4	10

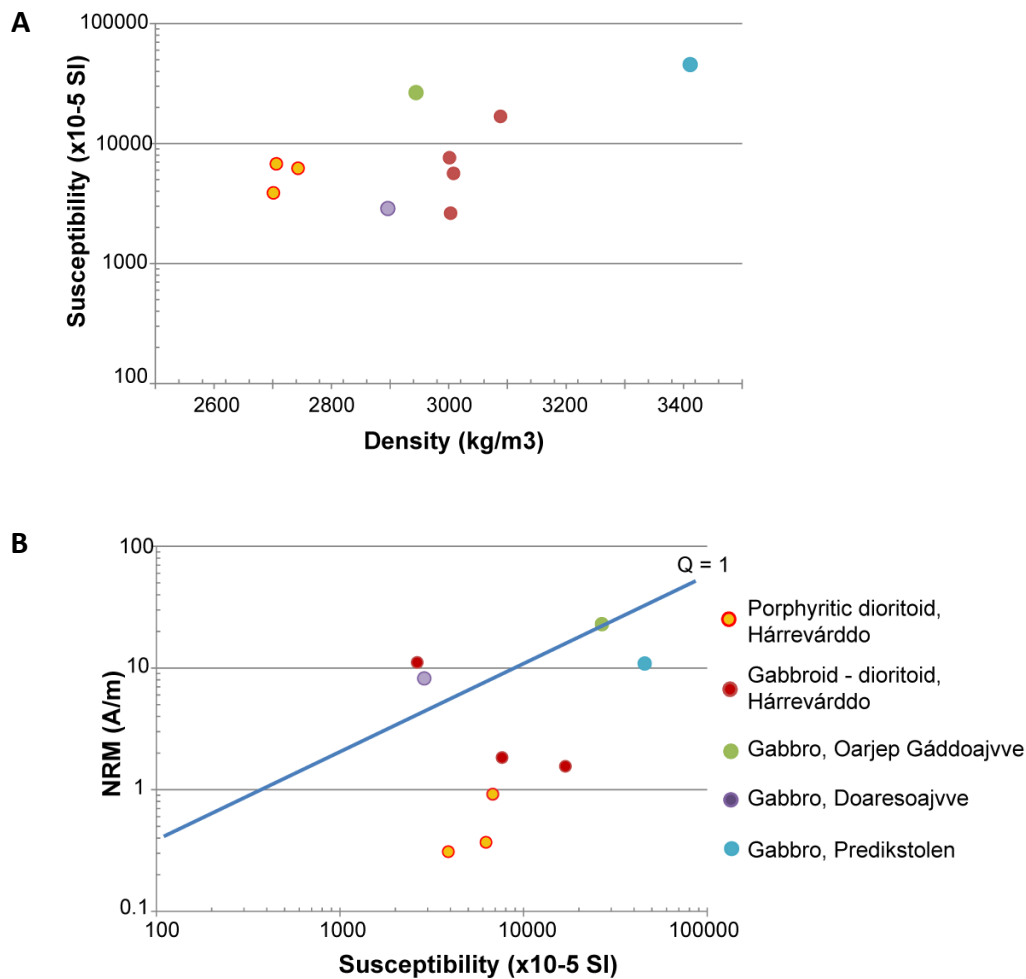


**Figure 12.** Variation of the petrophysical properties for gabbro-dioritoid samples from different parts, interpreted to be small intrusions within the Hárrevárddo intrusion. **A.** Density vs. magnetic susceptibility, **B.** magnetic susceptibility vs. remanent magnetisation (NRM).

## RESULTS OF 2.5D FORWARD GRAVITY AND MAGNETIC MODELLING

A profile for 2.5D modelling was chosen and the location across the Hárrevárddo intrusion is shown in figure 1B. The profile shows, using forward modelling of the gravity and magnetic data and in correspondence with measured foliation, a relatively steeply west-dipping contact in the east (fig. 13). The western contact to rocks of the same age but possibly predating the circular portion, shows a relatively steeply west-dipping contact, however no outcrops exist in that area. The internal contacts within the circular portion of the Hárrevárddo intrusion along the profile indicate steep, moderate, and flat dipping variation of contacts in the model (fig. 13). This is in accordance with the measurements at outcrops of the intrusion, which is variable with most from 8 to 65 degree dip angle.

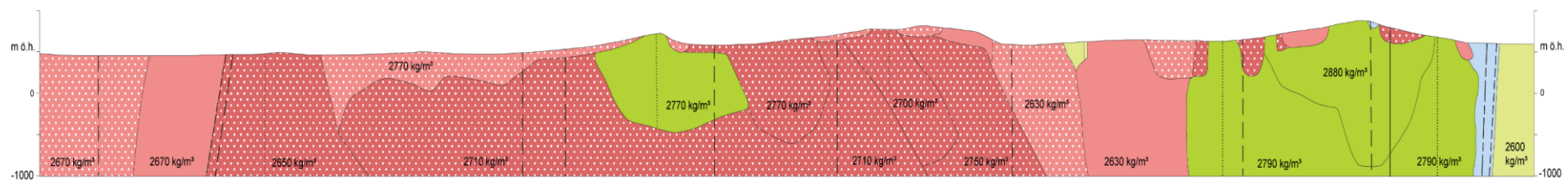


**Figure 13.** Profile from W to E along the black line shown in figure 1.

## GEOPHYSICAL 3D MODELLING

Geophysical cell-based modelling of the total magnetic field and Bouguer gravity fields has been carried out to study the shape, depth, and distribution of different anomalies in order to understand the subsurface geology for selected areas. We used the inverse technique described by Li & Oldenburg (1996, 1998) and Oldenburg & Pratt (2007) and refined our models by the use of parameter constraints from known susceptibility and density values from the study area. A regional trend was removed prior to the inversion.

### Modelling 3D gabbroid to dioritoid bodies using the magnetic field

A three-dimensional susceptibility model of the Hárrevárddo intrusion has been created with the inversion technique for selected areas where Geosoft Voxi software has been used. The model is divided into three-dimensional cells and the cells assigned susceptibility values that will reproduce the measured field.

Several samples of gabbroid to dioritoid rocks show susceptibility values above  $10\,000 \times 10^{-5}$  SI units and their density values range between  $2\,800$  and  $3\,400 \text{ kg/m}^3$ . The largest extent of gabbroid to dioritoid rocks are seen at the Hárrevárddo mountain, where they form the above mentioned high magnetic anomaly pattern with a  $4.5 \text{ km}$  diameter and produces a gravity surplus of  $6 \text{ mGal}$ . A three-dimensional susceptibility model has been constructed with inverse modelling technique in order to visualize the shape of this circular anomaly pattern at depth. The geographical position of the model area is shown with a black rectangle in figure 2. The cell sizes have been set to  $150 \times 150 \times 125$  meters in x, y, and z direction. The model has been restricted to susceptibility values between  $10$  and  $15\,000 \times 10^{-5}$  SI units. The obtained resulting model is displayed as an isosurface corresponding to a susceptibility of  $4\,000 \times 10^{-5}$  SI units and it shows steep sides on the east and southern part of the structure, while slightly dipping north on its northern part. The structure is similar to a so-called "ring dyke" with a depth of at least  $1\,000 \text{ m}$  (fig. 14).

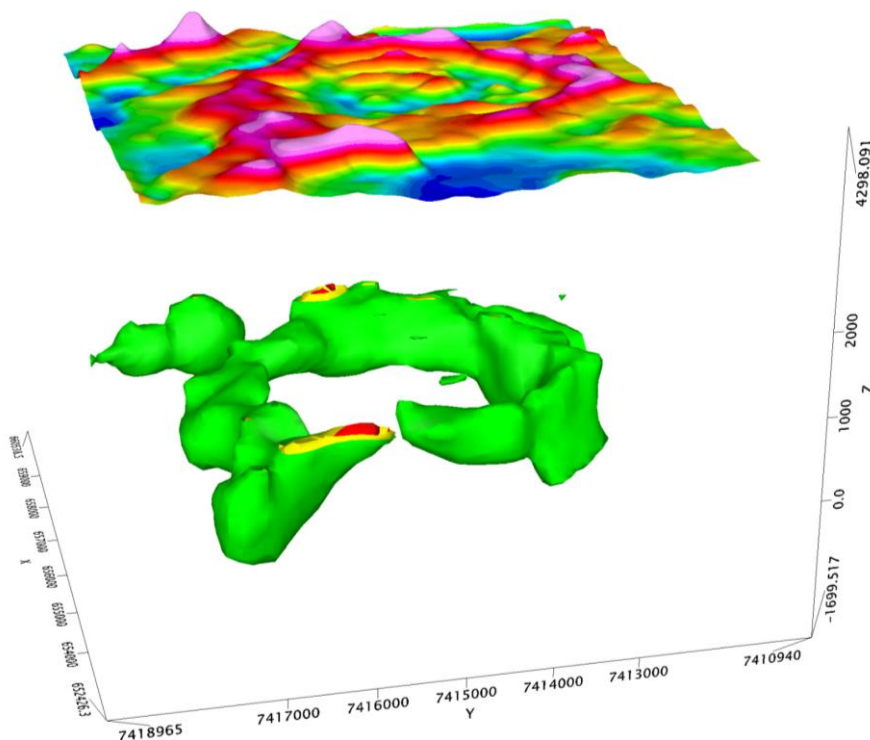


**Figure 14.** 3D susceptibility model of the "ring dyke" structure composed of gabbroid to dioritoid rocks. The area of the model is shown as a black rectangle in figure 2.

Small intrusions of basic magma with a diameter of  $\leq 1\,000$  m exist, e.g. at Oarjep Gáddoajvve in the southeastern part, just outside the Hárrevárddo intrusion (fig. 2). They demonstrate no metamorphic overprinting and are considered part of the magmatic events at around 1 784 Ma ago. These are typically high-magnetic rocks and despite high densities are difficult to detect on the gravity map because of the sparse measuring distance. At Oarjep Gáddoajvve there is a layered basic intrusion with plagioclase-rich parts and magnetite-rich parts, where a handheld compass misread significantly. The intrusion that has a diameter of 900 m is clearly visible on the magnetic anomaly map (fig. 2) and causes the highest magnetic anomaly in the airborne measurement within the study area. Susceptibility measurement at outcrops results in values of  $15\,000$  to  $25\,000 \times 10^{-5}$  SI units for magnetite-rich and biotite-bearing gabbroid to dioritoid (fig. 4N), and  $2\,500$  to  $3\,500 \times 10^{-5}$  SI units for plagioclase-rich gabbroid to dioritoid (fig. 4O). The gabbroic rocks at Oarjep Gáddoajvve are massive, well-preserved, and intrude older volcanic deposits (fig. 6O–V). Petrophysical measurement of a magnetite-rich gabbro sample shows susceptibility at  $27\,000 \times 10^{-5}$  SI units and density of  $3\,282$  kg/m<sup>3</sup>. A 3D susceptibility model with cell sizes  $50 \times 50 \times 25$  m and forced susceptibility values between  $10$  and  $40\,000 \times 10^{-5}$  SI has been created over the gabbro. The model area which is  $1.9 \times 1.35$  km is shown as a small rectangle in figure 2. The resulting model is visualized as a susceptibility isosurface  $> 20\,000 \times 10^{-5}$  SI and shows a clearly north plunging cylindrical structure with a minimum depth of 780 m (fig. 15). The model suggests a plug-like structure.

Southeast of the Hárrevárddo intrusion, beneath the lake Karats, there is another circular magnetic anomaly of about 1 km in diameter (fig. 2). Only one measuring point of gravity is located on the anomaly, which shows an elevation of the gravity field (fig. 3). One interpretation of the modelling of the magnetic field is that of a basic body at the surface, which dips towards the southeast (Antal Lundin *et al.* 2012b).

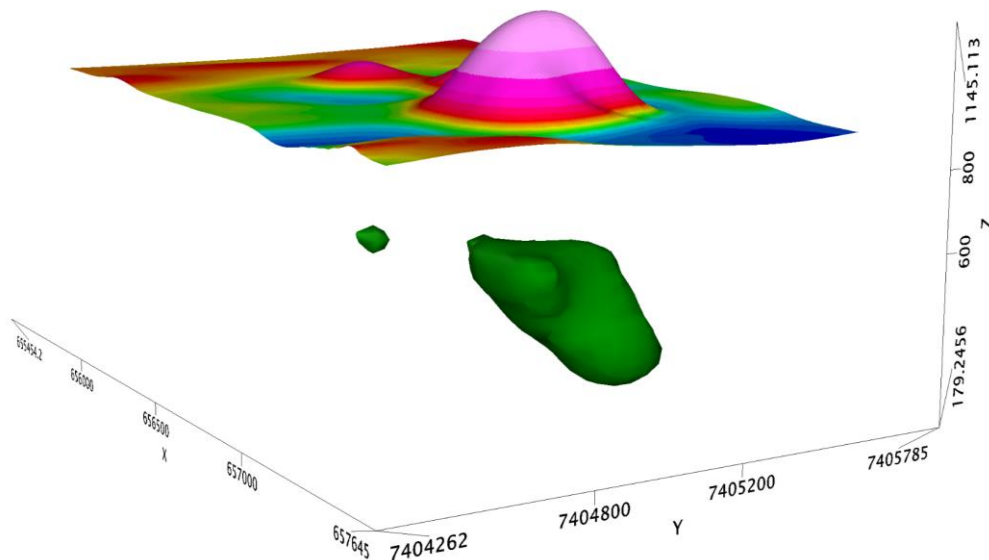


**Figure 15.** 3D model over a small, high susceptibility gabbro at Oarjep Gáddoajvve. The model is visualized as a susceptibility isosurface  $> 20\,000 \times 10^{-5}$  SI. The measured magnetic anomaly field is shown as a surface relief grid.

## Modelling the 3D internal structure using the gravity field

A 3D density model of the Hárrevárddo intrusion was created from the gravity field over the entire map area of  $33 \times 32$  km to explore the possible source geometries and density distributions (fig. 3). Before the modelling, a regional trend was removed from the Bouguer anomalies. For the model the cell size was set to  $500 \times 500 \times 250$  m in x, y, and z directions, respectively. To constrain the density model a density contrast between -0.07 and 0.34 was used, where 0 corresponds to  $2.67 \text{ g/cm}^3$ .

To improve the result a density constraint between  $2.60$  and  $3.50 \text{ g/cm}^3$  was set from known measured densities for petrophysical samples from the area. The density model is shown in figure 16. The total depth of the model from the topographical level is 6 900 m. As mentioned earlier an average density of  $2.70 \text{ g/cm}^3$  can explain the gravity surplus in the area and therefore, from the model, the created isosurfaces corresponds to  $2.70 \text{ g/cm}^3$ . They are shown with red colour in figure 16B visualizing the shape, depth, and distribution of rocks with densities of  $2.70 \text{ g/cm}^3$ . Isosurfaces corresponding to  $2.64 \text{ g/cm}^3$  are also shown with blue colour in figure 16B suggesting the presence of a large volume of low-density granites at depth as well. Corresponding measured density values of rocks from the Hárrevárddo intrusion is given in Table 2. The total volume for the density model corresponding to  $2.70 \text{ g/cm}^3$  is  $934 \text{ km}^3$ , slightly more than the total volume obtained for the low density isosurfaces which is  $800 \text{ km}^3$ .

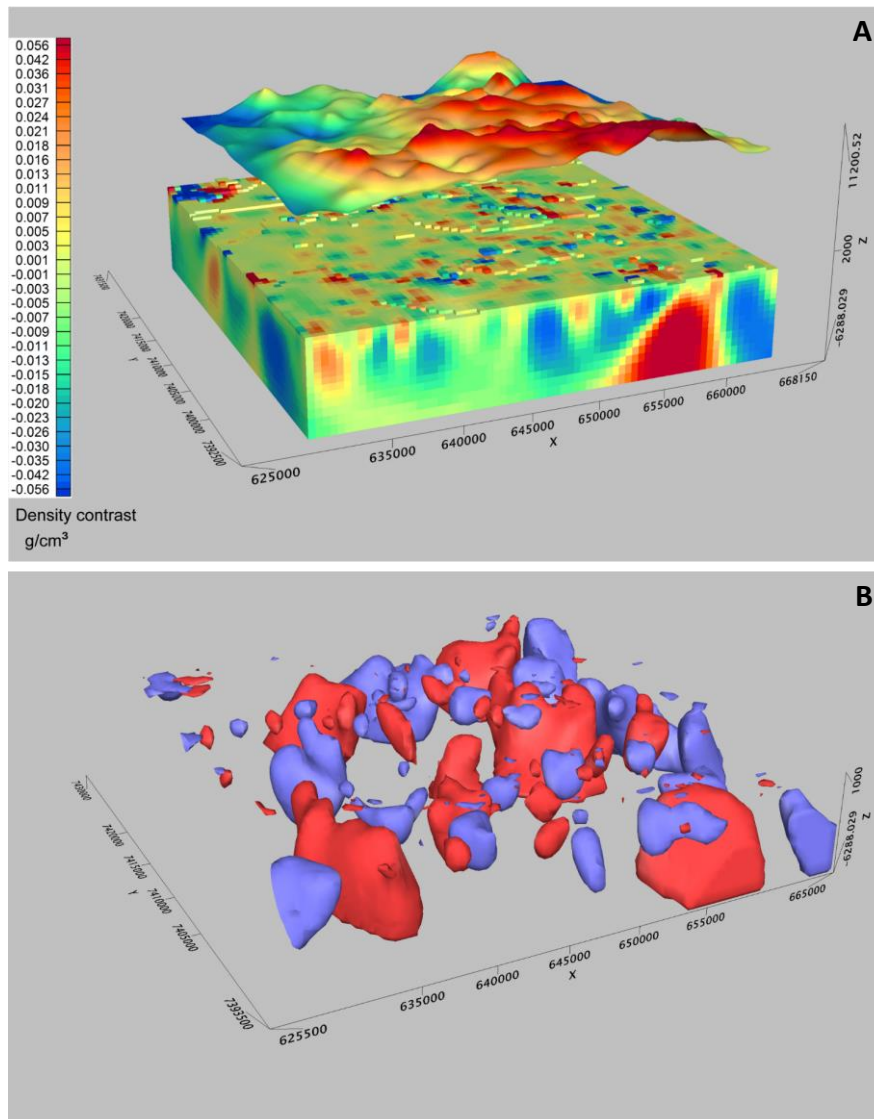


**Figure 16. A.** The 3D density model obtained after inversion of the gravity field. The gravity field as a relief surface is draped over the model. **B.** The 3D density model presented as isosurfaces corresponding to  $2.70 \text{ g/cm}^3$  (red) and  $2.64 \text{ g/cm}^3$  (blue). The model is created over the entire map area shown in figure 3.

## DISCUSSION

Magmatism often remains voluminous until the last stages of orogeny and the Hárrevárddo intrusion formed during the waning stages of the Svecokarelian orogeny in a continental arc-setting.

With an area of 500–800 km<sup>2</sup>, a modelled depth of at least 7 km resulting in 3 500–5 600 km<sup>3</sup> of magma, which would take an estimated 3.5 to 5.6 Ma to form using Saint Blanquat *et al.* (2011) compilation and a magma flux of 0.001 km<sup>3</sup>/year. If a faster rate at 0.01 km<sup>3</sup>/year is preferred it would still take 350 000–560 000 years. Faster than that is not probable, but a somewhat slower magma-feeding rate may be in accordance with the compilation by Saint Blanquat *et al.* (2011).

Since we envisage a relatively extended period of time in order to construct the Hárrevárddo intrusion, due to its size and multiple compositional character, a complex and heterogeneous magmatic process involving very different compositions and thermal regimes at depth with melting, segregation, transfer, and intermittent evolution in magma chambers at lower crustal positions, must have led to the final magma compositions that make up the Hárrevárddo intrusion (cf. Petford *et al.* 2000, Vigneresse & Clemens 2000, Cruden & McCaffrey 2001, Annen *et al.* 2015).

The geochemical characteristics of the different magmas within the Hárrevárddo intrusion must almost certainly have originated in a region of common melt generation, rather than result from *in-situ* processes at the emplacement level. The presence of different magma types with sharp internal contacts suggests that the geographical location, i.e. where the magmas end up is the common denominator rather than a single parent magma that fractionated *in-situ* (cf. Bergantz 2000, Glazner *et al.* 2004, Annen *et al.* 2015). Modelling suggests that melt generation is a major source of variation, and that other events that occur on the path to a shallower level within the crust and at the portion of the crust where the magma arrests its ascent, are second in importance to its source region (e.g. Annen *et al.* 2006, Solano *et al.* 2012, Annen *et al.* 2015).

The deduction from the geophysical modelling and sharp, but winding and wavy appearance of the contacts within the Hárrevárddo intrusion is that successive pulses intruded into partly solid rocks and partially molten but rigid rocks for the most part. This infers that the magma flux was episodic and not constant (cf. Annen *et al.* 2015, Schleicher & Bergantz 2017). Furthermore, the sharp contacts argue against a diapiric emplacement (e.g. Vigneresse & Clemens 2000). The lack of classical mingling or mixing structures may not indicate that none of these processes have occurred, just that these are not preserved in anything we have observed. The great number of different compositions of intrusive rocks in the Hárrevárddo intrusion and its size suggest the feasibility of mixing taking place. Recent numerical modelling of mixing processes indicate that it is rapid under the right conditions and identification of the process of mingling or mixing may become hard to find and observe, since they may be lost if the mixing is effective (e.g. Montagna *et al.* 2015, Schleicher *et al.* 2016, Schleicher & Bergantz 2017).

### Shape of gabbroid-dioritoid bodies

The different gabbroic magmas were not observed to have caused hybridized rocks with the felsic rocks within the Hárrevárddo intrusion that is seen in other bimodal complexes (e.g. Délérís 1996, Wiebe *et al.* 2004). Recognizing multiple pulses within plutons is only uncomplicated when a major compositional difference exists or appearance of the rocks differ, and the age relations are easily discerned at the outcrops. Bimodal magmatism and related interaction, and mixing of rocks, are reported in several structurally complex and simpler intrusions, and theoretically investigated (e.g. Délérís *et al.* 1996, Bergantz 2000, Meade *et al.* 2014).

According to the gravity data there are no major mafic magmas down to a depth of c. 7 km (fig. 3, 16). Magnetic modelling shows that the “ring-dyke” structure of gabbroic rocks at the Hárrevárddo mountain continues to a depth of at least 1 km (fig. 14).

Classical ring dykes may form when a caldera collapses and this is due to relatively rapid emptying of its magma chamber (e.g. Richey & Thomas 1930, O'Driscoll *et al.* 2006). Following the discharge of vast amounts of magma, subsidence and fracturing occurs with formation of ring faults that are vertical to steeply dipping. These ring faults are the conduits that allow magma from beneath to rise, forming a ring dike or cone sheets depending on depth (e.g. Burchardt *et al.* 2013, Galland *et al.* 2014). The measurements of contacts between basic rocks of the Hárrevárddo “ring dyke” structure and acidic rocks show plunges from 60 to 80 degrees. The 2.5 modelling indicate that the contacts may even have steeper dip at depth (fig. 13). These observations and the modelling are in agreement with a classical ring dyke formed due to a caldera collapse. If there was a caldera collapse at Hárrevárddo, part of the resulting volcanic rocks could be the recently discovered volcanic successions at Tjåkkaure about 28 km towards SE, as pointed out by Claeson & Antal Lundin (2019). The age determined trachybasaltic andesite to andesite from Tjåkkaure at  $1\,773 \pm 7$  Ma is more or less coeval with the rocks of the Hárrevárddo intrusion and lithochemical data is in accordance with a possible affinity (Claeson *et al.* 2018a).

The ring-shape of the gabbroic rocks at Hárrevárddo is complex, it may have had this shape while intruding the solid felsic rocks. There is also a difference within the gabbro, porphyritic at outcrops to the north and even-grained gabbro to the south, which indicate that it is not a simple gabbroic layer. One interpretation is that the “ring-dyke” structure is made of different pulses with different compositions. Another that the feldspar porphyritic part of the gabbroic rocks was at a higher level where the lighter minerals floated to, alternatively the distribution of phenocrysts is due to flow-induced differentiation while moving. The two latter interpretations invoke that it is a single mafic magma injection to start off with. We also described above that at Hárrevárddo there are layering features among the different gabbroic compositions in the ring-shaped structure that plunge around 65 degrees. The layering is even seen in different weathering characteristics due to mineralogical differences between layers (fig. 4H, 6G–L).

### **Laccolith versus lopolith shape and form of incremental pulses of magma**

For laccolith-shaped intrusions the consensus is that such intrusions are rarely emplaced deeper than 3 km and for the most part at a higher position (e.g., Corry 1988). In order to form a laccolith shape, deflection and roof lifting of the overburden has to be widespread and probably over most of the intrusion's width (e.g. Corry 1988, Petford *et al.* 2000, Currier & Marsh 2015, and references therein). A suggested critical radius of the intrusion of c. 3.3 times the thickness of the overburden makes large intrusions close to the surface more likely to form laccolith-shaped intrusions (Pollard & Johnson 1973, Currier & Marsh 2015). The recent work of Currier & Marsh (2015) demonstrates that along with deflection of the overburden there has to be a large resistance at the intrusion margin. High magma viscosity is proposed to be important, because of either composition or cooling, and necessary to supply the critical flow resistance to induce inflation (Currier & Marsh 2015). The fracture toughness of the host rock is another controlling factor for laccolith-shaped intrusions (e.g. Corry 1988, Bungler & Cruden 2011, Cruden *et al.* 2018). The metamorphic overprinting of the surrounding rocks indicates a depth of at least 11 km of overburden at some point at the Hárrevárddo intrusion. The radius of the Hárrevárddo intrusion at the exposed level is c. 13 km and the estimated thickness from gravity data is at least c. 7 km, and then there is an unknown roof section that is gone. The topography of the exposed Hárrevárddo intrusion shows that a thickness of at least 700 m is exposed in vertical direction. The semi-circular shape seen in the magnetic data of the Hárrevárddo intrusion (fig. 2) strongly implies that magma propagation must have occurred over most of its perimeter and been close to constant in all directions, otherwise different shapes are expected (cf. Currier & Marsh 2015). All the above consequently discard a possible laccolith shape for the Hárrevárddo intrusion.

In recent decades the identification of tabular laccoliths and plutons formed through incremental injections of magma instead of plutonic diapirs has led to fundamental reinterpretations and some that still favour diapirism (e.g. Vigneresse & Clemens 2000, Cruden & McCaffrey 2001, Glazner *et al.* 2004, Cottam *et al.* 2010, Paterson *et al.* 2011). Laccoliths and plutons do not have exactly the same power-law exponents when studying the relationship between vertical thickness and horizontal length, which is attributed to differences in mechanical behaviour (Petford *et al.* 2000) and the accounts for the weight of the magma, deformation of the overburden according to thin elastic plate theory, and propagation according to linear elastic fracture mechanics (Bunger & Cruden 2011, Cruden *et al.* 2018). Experiments show the importance of the time-dependent events associated with igneous intrusions (cf. Bunger & Cruden 2011, Currier & Marsh 2015, Currier *et al.* 2017, Cruden *et al.* 2018). Incremental accumulation and intermittent growth of igneous bodies occurs over various timescales (e.g. Glazner *et al.* 2004, Menand 2008, Horsman *et al.* 2010, Annen 2011, Zieg & Marsh 2012, Annen *et al.* 2015, Sparks & Cashman 2017). These experiments and studies show that even a single emplacement pulse of magma is a complicated process. The thickness of the Hárrevárddo intrusion, geophysically modelled shapes of different lithologies within and the intrusion itself, suggest a resemblance of several incremental injections of differently sized magma pulses of different tabular shapes, forming a lopolith with floor depression (fig. 1–3, 14–16). The lopolith shape with floor depression is also consistent with the interpreted ring dyke.

Diapiric emplacement is a buoyancy-driven density-contrast process that requires the imposition of significant strain on the already intruded rock volume. Such deformation is not observed in the Hárrevárddo intrusion. In fact, the presence of sharp contacts strongly argues against a diapiric emplacement process and would rather suggest emplacement via sheets or irregularly tabular-shaped pulses of magma.

### **Regional stress-field during emplacement and cooling**

The large size of the Hárrevárddo intrusion ensures that the tectonic record at the time of construction is preserved (cf. Saint Blanquat *et al.* 2011). The Hárrevárddo intrusion is thus formed during regional extension and in absence of a regional compressional tectonic-deformation field or a rather weak one. The parallel to subparallel magmatic-flow structures and foliations pattern to the outer contact as well as the more flat-lying planar structures in the more central parts, giving a notion of a domal shape of the Hárrevárddo intrusion (fig. 9), are indicative of no major regional syn-magmatic compressional deformation (e.g. Saint Blanquat *et al.* 2011). The airborne magnetic data show particularly well how the Hárrevárddo intrusion cuts and drapes all rocks on its outer perimeter (fig. 2, 9). The draping and deformation are most probably mainly due to magma push during inflation and floor depression (e.g. Cruden 2006, 2008). Furthermore, the foliations of the Hárrevárddo intrusion cuts and is discordant at the regional scale but concordant on the scale of the intrusion (fig. 8, 9). Alternatively, the Hárrevárddo intrusion formed faster than any regional stress field could be recorded. Since the key timescale is that of the emplacement and solidification of individual pulses, which can be orders of magnitude faster than the accumulation rate of regional tectonic strain, but this hypothesis is less likely due to the size of the Hárrevárddo intrusion and the time it will take to form (see above). Thus, the more favourable hypothesis is that the structures are related to the formation of the intrusion during an extensional setting, which lacks any record of other contemporaneous regional deformation (fig. 8, 9). A compressional setting is less plausible due to the above observations and this is also further shown by the regional foliation and lineation patterns that show no correlation with those seen within the Hárrevárddo intrusion or its immediate host rocks (fig. 8, 9, Claeson & Antal Lundin 2019). An extensional setting that also provides space accommodation of the pulses of magma to form the Hárrevárddo intrusion is reasonable.

In continental magmatic-arc settings extension is common and during the evolution of a continental arc it may shift in the upper plate between extensional, compressional, or neutral (e.g. Grocott *et al.* 2009, Ducea *et al.* 2015). However, if there was fault-assisted vertical pluton growth in this case, as shown in Grocott *et al.* (2009), has not been established and left to future research.

## CONCLUSIONS

Magmatism often remains voluminous until the last stages of orogeny and the Hárrevárddo intrusion most probably formed in an extensional setting, during the waning stages of the Svecokarelian orogeny in a continental-arc setting.

Successive injection of magma pulses is plausible as the fundamental process essential to construction of the Hárrevárddo intrusion. Several incremental injections of differently sized magma pulses are envisaged from the field observations, lithogeochemical data and geophysical modelling. The magma pulses were of very different compositions and had different amounts of phenocrysts, indicating a complex set of magmas and chambers in the melt generation area at greater depth within the crust.

No previous mapping effort has recognized that the Hárrevárddo intrusion may be considered as a large or structurally complex intrusion, with associated bimodal magmatism. The Hárrevárddo intrusion comprise a Paleoproterozoic late-Orosirian to early-Statherian magmatism of the Svecokarelian orogen that may in future research be used as a case study that allows us to study magmatic processes and pluton growth in detail without major tectonic interference from that era.

## ACKNOWLEDGEMENTS

Reviews by A.R. Cruden and T.M. Rasmussen are much appreciated and significantly improved the manuscript.

This work was supported by the Geological Survey of Sweden through an internal research grant, project 35291.

## REFERENCES

- Annen, C., 2011: Implications of incremental emplacement of magma bodies for magma differentiation, thermal aureole dimensions and plutonism-volcanism relationships. *Tectonophysics* 500, 3–11.
- Annen, C., Blundy, J.D., Leuthold, J. & Sparks, R.S.J., 2015: Construction and evolution of igneous bodies: Towards an integrated perspective of crustal magmatism. *Lithos* 230, 206–221.
- Annen, C., Blundy, J.D. & Sparks, R.S.J., 2006: The genesis of intermediate and silicic magmas in deep crustal hot zones. *Journal of Petrology* 47, 505–539.
- Antal Lundin, I., Claeson, D., Hellström, F. & Kero, L., 2010: Sydvästra Norrbotten. In H. Delin (ed.): Berggrundsgeologisk undersökning. Sammanfattning av pågående verksamhet 2009. *SGU-rapport 2010:2*, Sveriges geologiska undersökning, 43–69.
- Antal Lundin, I., Claeson, D. & Hellström, F., 2011: Sydvästra Norrbotten, berg. In S. Lundqvist (ed.): Sammanfattning av pågående verksamhet 2010. Berggrundsgeologisk undersökning. *SGU-rapport 2011:6*, Sveriges geologiska undersökning, 86–105.
- Antal Lundin, I., Claeson, D., Hellström, F. & Berggren, R., 2012a: Berggrundsgeologisk undersökning, sydvästra Norrbotten. Sammanfattning av pågående verksamhet 2011. *SGU-rapport 2012:3*, Sveriges geologiska undersökning, 1–34.
- Antal Lundin, I., Claeson, D., Hellström, F. & Berggren, R., 2012b: Berggrundsgeologisk undersökning, sydvästra Norrbotten. Sammanfattning av pågående verksamhet 2012. *SGU-rapport 2012:21*, Sveriges geologiska undersökning, 1–44.
- Aster, R.C., Borchers, B. & Thurber, C.H., 2005: *Parameter estimation and inverse problems*. Academic Press, 1–320.
- Bergantz, G.W., 2000: On the dynamics of magma mixing by reintrusion: implications for pluton assembly processes. *Journal of Structural Geology* 22, 1297–1309.
- Boynnton, W.V., 1984: Cosmochemistry of the Rare Earth Elements: Meteorite studies. In P. Henderson (ed.), *Rare earth element geochemistry*. Elsevier Science B.V., 63–114.
- Bucher, K. & Frey, M., 1994: *Petrogenesis of metamorphic rocks*. 6th Edition complete revision of Winkler's textbook. Springer-Verlag, 1–318.
- Bunger, A.P. & Cruden, A.R., 2011: Modeling the growth of laccoliths and large mafic sills: the role of magma body forces. *Journal of Geophysical Research* 116, B02203, 1–18. DOI:10.1029/2010JB007648.
- Burchardt, S., Troll, V.R., Mathieu, L., Emeleus, H.C. & Donaldson, C.H., 2013: Ardnamurchan 3D cone-sheet architecture explained by a single elongate magma chamber. *Scientific Reports* 3, 2891; DOI:10.1038/srep02891.
- Burton-Johnson, A., Macpherson, C.G. & Hall, R., 2016: Internal structure and emplacement mechanism of composite plutons: evidence from Mt Kinabalu, Borneo. *Journal of the Geological Society* 174, 180–191.
- Claeson, D. & Antal Lundin, I., 2013: Berggrundsgeologisk undersökning, sydvästra Norrbotten. Sammanfattning av pågående verksamhet 2013. *SGU-rapport 2013:18*, Sveriges geologiska undersökning, 1–27.
- Claeson, D., Antal Lundin, I., 2015. Berggrundsgeologisk undersökning, sydvästra Norrbotten. Sammanfattning av pågående verksamhet 2014. *SGU-rapport 2015:03*, Sveriges geologiska undersökning, 1–32.
- Claeson, D. & Antal Lundin, I., 2019: Beskrivning till berggrundskartorna Tjåmotis SV och SO. *Sveriges geologiska undersökning K625*, 1–64.

- Claeson, D., Antal Lundin, I. & Hellström, F., 2018a New volcanic succession at 1.77 Ga determined by U-Pb zircon age of andesitoid at Tjåkkaure, map sheet 27I Tjåmotis SO, Norrbotten County. *In* D. Claeson & I. Antal Lundin (eds.): U-Pb zircon geochronology of rocks from the mid and southwestern part of Norrbotten County, Sweden. *SGU-rapport 2018:22*, Sveriges geologiska undersökning, 196–207.
- Claeson, D., Antal Lundin, I. & Hellström, F., 2018b: U-Pb zircon age determination of the Hárrevårdö intrusion using quartz monzonite at Jervas, map sheet 27I Tjåmotis SV, Norrbotten County. *In* D. Claeson & I. Antal Lundin (eds.): U-Pb zircon geochronology of rocks from the mid and southwestern part of Norrbotten County, Sweden. *SGU-rapport 2018:22*, Sveriges geologiska undersökning, 171–185.
- Claeson, D., Antal Lundin, I. & Hellström, F., 2018c: U-Pb zircon age of monzonite at Njuorramjauratj, map sheet 27J Porjus SV, Norrbotten County. *In* D. Claeson & Antal Lundin (eds.): U-Pb zircon geochronology of rocks from the mid and southwestern part of Norrbotten County, Sweden. *SGU-rapport 2018:22*, Sveriges geologiska undersökning, 106–115.
- Corry, C.E., 1988: *Laccoliths: Mechanics of emplacement and growth*. Geological Society of America, Special Paper 220, 1–110.
- Cottam, M., Hall, R., Sperber, C. & Armstrong, R., 2010: Pulsed emplacement of the Mount Kinabalu granite, northern Borneo. *Journal of the Geological Society* 167, 49–60.
- Cruden, A.R., 2006: Emplacement and growth of plutons: implications for rates of melting and mass transfer in continental crust. *In* M. Brown & T. Rushmer (eds.): *Evolution and Differentiation of the Continental Crust*. Cambridge University Press, 455–519.
- Cruden, A.R., 2008: Emplacement mechanisms and structural influences of a younger granite intrusion into older wallrocks – a principal study with application to the Götömar and Uthammar granites. *SKB Rapport R-08-138*, Svensk Kärnbränslehantering AB, 1–48.
- Cruden, A.R. & McCaffrey, K.J.W., 2001: Growth of plutons by floor subsidence: Implications for rates of emplacement, intrusion spacing and melt-extraction mechanisms. *Physics and Chemistry of the Earth, Part A: Solid Earth and Geodesy* 26, 303–315.
- Cruden, A.R. McCaffrey, K.J.W. & Bungler, A.P., 2018: Geometric scaling of tabular igneous intrusions: implications for emplacement and growth. *In* C. Breitkreuz & S. Rocchi, S. (eds.): *Physical Geology of Shallow Magmatic Systems - Dykes, Sills and Laccoliths*. Springer, 11–38.
- Currier, R.M., Forsythe, P., Grossmeier, C., Laliberte, M. & Yagle, B., 2017: Experiments on the evolution of laccolith morphology in plan-view. *Journal of Volcanology and Geothermal Research* 336, 155–167.
- Currier, R.M. & Marsh, B.D., 2015: Mapping real time growth of experimental laccoliths: The effect of solidification on the mechanics of magmatic intrusion. *Journal of Volcanology and Geothermal Research* 302, 211–224.
- Debon, F., 1980: Genesis of the three concentrically-zoned granitoid Plutons of Caunterets-Panticosa (French and Spanish Western Pyrenees). *Geologische Rundschau* 69, 107–130.
- Déléris, J., Nédélec, A., Ferré, E., Gleizes, G., Ménot, R.-P., Obasi, C.K. & Bouchez, J.-L., 1996: The Pan-African Toro Complex (northern Nigeria): magmatic interactions and structures in a bimodal intrusion. *Geological Magazine* 133, 535–552.
- Ducea, M.N., Saleeby, J.B. & Bergantz, G., 2015: The Architecture, Chemistry, and Evolution of Continental Magmatic Arcs. *Annual Review of Earth and Planetary Sciences* 43, 299–331.
- Galland, O., Burchardt, S., Hallot, E., Mourgues, R., Bulois, C., 2014: Dynamics of dikes versus cone sheets in volcanic systems. *Journal of Geophysical Research: Solid Earth*, 2014JB011059, DOI:10.1002/2014jb011059.
- Gerbi, C., Johnson, S.E. & Paterson, S.R., 2004: Implications of rapid, dike-fed pluton growth for host-rock strain rates and emplacement mechanisms. *Journal of Structural Geology* 26, 583–594.

- Glazner, A.F., Bartley, J.M., Coleman, D.S., Gray, W. & Taylor, R.Z., 2004: Are plutons assembled over millions of years by amalgamation from small magma chambers? *GSA Today* 14, 4–11.
- Gleizes, G., Leblanc, D., Santana, V., Olivier, P. & Bouchez, J.L., 1998: Sigmoidal structures featuring dextral shear during emplacement of the Hercynian granite complex of Caunterets–Panticosa (Pyrenees). *Journal of Structural Geology* 20, 1229–1245.
- Gil-Imaz, A., Lago-San José, M., Galé, C., Pueyo-Anchuela, Ó., Ubide, T., Tierz, P. & Oliva-Urcia, B., 2012: The Permian mafic dyke swarm of the Panticosa pluton (Pyrenean Axial Zone, Spain): simultaneous emplacement with the late-Variscan extension. *Journal of Structural Geology* 42, 171–183.
- Grocott, J., Arevalo, C., Welkner, D. & Cruden, A.R., 2009: Fault-assisted vertical pluton growth: Coastal Cordillera, northern Chilean Andes. *Journal of the Geological Society of London*, 166, 295–301.
- Horsman, E., Morgan, S., Saint-Blanquat, M. (de), Habert, G., Nugent, A., Hunter, R.A. & Tikoff, B., 2009: Emplacement and assembly of shallow intrusions from multiple magma pulses, Henry Mountains, Utah. *Earth and Environmental Science Transactions of the Royal Society of Edinburgh* 100, 117–132.
- Le Maitre, R.W. (ed.), Streckeisen, A., Zanettin, B., Le Bas, M.J., Bonin, B., Bateman, P., Bellieni, G., Dudek, A., Efremova, S., Keller, J., Lameyre, J., Sabine, P.A., Schmid, R., Sörensen, H. & Woolley, A.R., 2002: *Igneous rocks: IUGS classification and glossary: recommendations of the International Union of Geological Sciences, Subcommission on the Systematics of Igneous Rocks. 2nd ed.* Cambridge University Press, 1–236.
- Li, Y. & Oldenburg, D.W., 1996: 3D inversion of magnetic data. *Geophysics* 61, 394–408.
- Li, Y. & Oldenburg, D.W., 1998: 3D inversion of gravity data. *Geophysics* 63, 109–119.
- Meade, F.C., Troll, V.R., Ellam, M., Freda, C., Font, L., Donaldson, C.H. & Klonowska, I., 2014: Bimodal magmatism produced by progressively inhibited crustal assimilation. *Nature Communications* 5:4199, doi: 10.1038/ncomms5199.
- Menand, T., 2008: The mechanics and dynamics of sills in layered elastic rocks and their implications for the growth of laccoliths and other igneous complexes. *Earth and Planetary Science Letters* 267, 93–99.
- Montagna, C.P., Papale, P. & Longo, A., 2015: Timescales of mingling in shallow magmatic reservoirs. In L. Caricchi & J.D. Blundy (eds.): *Chemical, Physical and Temporal Evolution of Magmatic Systems*. Geological Society of London, Special Publications 422, 131–140.
- Nédélec, A. & Bouchez, J.-L., 2015: *Granites: Petrology, Structure, Geological Setting, and Metallogeny*. Oxford University Press, 1–335.
- Nysten, P., Persson, S. & Triumpf, C.-T., 2014: Barentsprojektet 2013: Berggrundsgeologisk undersökning 27I Tjåmotis NV och NO. *SGU-rapport 2014:11*, Sveriges geologiska undersökning, 1–30.
- O’Driscoll, B., Troll, V.R., Reavy, R.J. & Turner, P., 2006: The great eucrite intrusion of Ardnamurchan, Scotland: reevaluating the ring-dike concept. *Geology* 34, 189–192.
- Oldenburg, D.W. & Pratt, D.A., 2007: Geophysical inversion for mineral exploration: a decade of progress in theory and practice. In B. Milkereit (ed.): *Proceedings of Exploration ’07: Fifth Decennial Mineral Exploration Conference on Mineral exploration*. Decennial Mineral Exploration Conferences, 61–95.
- Paterson, S.R., Okaya, D., Memeti, V., Economos, R. & Miller, R.B., 2011: Magma addition and flux calculations of incrementally constructed magma chambers in continental margin arcs: Combined field, geochronologic, and thermal modeling studies. *Geosphere* 7, 1439–1468.
- Petford, N., Cruden, A.R., McCaffrey, K.J.W. & Vigneresse, J.-L., 2000: Granite magma formation, transport and emplacement in the Earth’s crust. *Nature* 408, 669–673.

- Pollard, D.D. & Johnson, A.M., 1973: Mechanics of Growth of some Laccolithic Intrusions in the Henry Mountains, Utah, II. *Tectonophysics* 18, 311–354.
- Razanatseho, M.O.M., Nédélec, A., Rakotondrazafy, M., Meert, J.G. & Ralison, B., 2009: Four-stage building of the Cambrian Carionpluton (Madagascar). *Earth and Environmental Science Transactions of the Royal Society of Edinburgh* 100, 133–145.
- Richey, J.E. & Thomas, H.H., 1930: *The Geology of Ardnamurchan, North-west, Mull and Coll*. Memoir of the Geological Survey of Great Britain [Scotland], HMSO, 1–393.
- Saint Blanquat, M. (de), Horsman, E., Habert, G., Morgan, S., Vanderhaeghe, O., Law, R. & Tikoff, B., 2011: Multiscale magmatic cyclicality, duration of pluton construction, and the paradoxical relationship between tectonism and plutonism in continental arcs. *Tectonophysics* 500, 20–33.
- Schleicher, J.M. & Bergantz, G.W., 2017: The Mechanics and Temporal Evolution of an Open-system Magmatic Intrusion into a Crystal-rich Magma. *Journal of Petrology* 58, 1059–1072.
- Schleicher, J.M., Bergantz, G.W., Breidenthal, R.E. & Burgisser, A., 2016: Time scales of crystal mixing in magma mushes. *Geophysical Research Letters* 43, 1543–1550.
- Solano, J.M.S., Jackson, M.D., Sparks, R.S.J., Blundy, J.D. & Annen, C., 2012: Melt segregation in deep crustal hot zones: a mechanism for chemical differentiation, crustal assimilation and the formation of evolved magmas. *Journal of Petrology* 53, 1999–2026.
- Sparks, R.S.J. & Cashman, K.V., 2017: Dynamic magma systems: Implications for forecasting volcanic activity. *Elements* 13, 35–40.
- Sun, S.S. & McDonough, W.F., 1989: Chemical and isotopic systematic of oceanic basalts: implications for mantle composition and processes. In A.D. Saunders & M.J. Norry (eds.): *Magmatism in ocean basins*. Geological Society of London, Special Publication 42, 313–345.
- Vigneressse, J.-L. & Clemens, J.D., 2000: Granitic magma ascent and emplacement: neither diapirism nor neutral buoyancy. In B. Vendeville, Y. Mart, & J.-L. Vigneressse (eds.): *Salt, Shale and Igneous Diapirs in and around Europe*. Geological Society of London, Special Publication 174, 1–19.
- Whitney, D.L. & Evans, B.W., 2010: Abbreviations for names of rock-forming minerals. *American Mineralogist* 95, 185–187.
- Wiebe, R.A., Manon, M.R., Hawkins, D.P. & McDonough, W.F., 2004: Late-stage mafic injection and thermal rejuvenation of the Vinalhaven Granite, Coastal Maine. *Journal of Petrology* 45, 2133–2153.
- Zieg, M.J. & Marsh, B.D., 2012: Multiple reinjections and crystal-mush compaction in the Beacon Sill, McMurdo Dry Valleys, Antarctica. *Journal of Petrology* 53, 2567–2591.